HHS Public Access

Author manuscript

J Immunol. Author manuscript; available in PMC 2024 February 01.

Published in final edited form as:

J Immunol. 2023 February 01; 210(3): 259–270. doi:10.4049/jimmunol.2200487.

Lung resident memory T cells activated by oral vaccination afford comprehensive protection against pneumonic *Yersinia pestis* infection

Amit K. Singh[†], **Saugata Majumder**[†], **Xiuran Wang**[†], **Renjie Song**[#], **Wei Sun**[†]

[†]Department of Immunology and Microbial Disease, Albany Medical College, Albany, NY, 12208, USA

[#]Immunology Core at Wadsworth Center, New York State Department of Health, Albany, NY, 12208, USA

Abstract

A growing body of evidence has shown that resident memory T (T_{RM}) cells formed in tissue following mucosal infection or vaccination are crucial for counteracting reinfection by pathogens. However, whether lung T_{RM} cells activated by oral immunization with Yptb1(pYA5199) play a protective role against pneumonic plague remains unclear. In this study, we demonstrated that lung $CD4^+$ and $CD8^+$ T_{RM} cells significantly accumulated in the lungs of orally Yptb1(pYA5199)-vaccinated mice, and dramatically expanded with elevated IL-17A, IFN-γ, and/or TNF-α production following pulmonary *Yersinia pestis* infection and afforded significant protection. Short-term or long-term treatment of immunized mice with FTY720 did not affect lung T_{RM} cell formation and expansion, or protection against pneumonic plague. Moreover, the intratracheal transfer of both lung $CD4^+$ and $CD8^+$ T_{RM} cells conferred comprehensive protection against pneumonic plague in naïve recipient mice. Lung T_{RM} cell-mediated protection was dramatically abolished by the neutralization of both IFN-γ and IL-17A. Our findings reveal that lung T_{RM} cells can be activated via oral Yptb1(pYA5199) vaccination and that IL-17A and IFN-γ production play an essential role in adaptive immunity against pulmonary *Y. pestis* infection. This study highlights an important new target for developing an effective pneumonic plague vaccine.

Keywords

Y. pseudotuberculosis ; oral immunization; mucosal immunity; lung resident memory T cells; pneumonic plague

Corresponding author: Wei Sun, Department of Immunology and Microbial Disease, Albany Medical College, Albany, NY, 12208, USA. sunw@amc.edu.

Contributions: Experiments conceived and designed by AKS and WS; experiments performed by AKS, SM, XRW, and RS; data analyzed by AKS and WS; manuscript written by AKS and WS and edited by WS.

Conflict of interest: All authors declare that they have no conflicts of interest.

Introduction

Pneumonic plague, caused by pulmonary *Yersinia pestis* infection, is a rapidly progressing disease with ~60% mortality with prompt treatment and almost 100% mortality if treatment is delayed beyond 24 hours (1, 2). Due to the high fatality rate, the potential use of plague as a biological weapon is of great concern (3). In recent decades, only a few thousand cases have been reported annually around the world, leading to the disregard of past great devastation caused by the plague in human history (4). However, changes in the climate and environment, host and vector species, and human territory have recently been connected with several large regional plague outbreaks (2). Moreover, the emergence of multidrug-resistant *Y. pestis* is another cause for increasing concern regarding this deadly agent (4). Therefore, developing a vaccine capable of preventing a repeat of historical tragedies or providing effective protection against potential terroristic attacks is imperative. However, there is no licensed plague vaccine recommended by the WHO (5). Additionally, current challenges highlight the need for a better understanding of protective immune mechanisms to develop new vaccines that provide comprehensive protection.

Recently, the dogma of memory T cells included the subdivision of these cells into three subsets: (1) central memory T (T_{CM}) cells marked with $CD62L^+$ that can circulate to secondary lymphoid organs, where they can differentiate into effector T cells in response to antigen stimulation; (2) effector memory T (T_{EM}) cells marked with $CD62L^-$ $CD44^+$ that can migrate to inflamed peripheral nonlymphoid tissues (NLTs), such as the skin, gut, and lungs, and display immediate effector function (6, 7); and (3) a newly discovered T-cell subset, tissue-resident memory T (T_{RM}) cells marked with $CD69^+$ and/or $CD103^+$ (αEβ7 integrin) that can reside in peripheral tissues but lose the ability to recirculate (8). An increasing number of studies have demonstrated that lung $CD4^+$ and/or $CD8^+$ T_{RM} cells activated by mucosal vaccination can mediate protection against bacterial/viral infection at lung mucosal sites (9-12).

Previous studies have demonstrated that protection against pulmonary *Y. pestis* infection mainly requires $CD4^+$ and/or $CD8^+$ T cells, which are characterized by the production of IFN-γ, TNF-α, and IL-17A (13-15). In our previous study, oral vaccination with the live attenuated *Y. pseudotuberculosis* (Yptb) strain χ10069(pYA5199), which was engineered with Δ*asd* Δ*yopK* Δ*yopJ* triple mutations and used to deliver the *Y. pestis* fusion protein $YopE_{Nt138}$-LcrV, activated *Y. pestis*-specific lung $CD4^+$ and $CD8^+$ T cells producing high levels of IFN-γ, TNF-α, and IL-17A in immunized mice, which provided significant protection against pulmonary *Y. pestis* infection (16). However, whether the defined T-cell subclass, such as lung T_{RM} cells, can be elicited by oral vaccination with an attenuated Yptb strain and confer protection against pneumonic plague has not been appreciated. In this study, we used a newly constructed Yptb strain, Yptb1(pYA5199), incorporating the *Y. pestis caf1* operon encoding the F1 antigen as an oral vaccine to evaluate the roles of lung T_{RM} cells in protection against pneumonic plague in outbred Swiss Webster mice.

Materials and Methods

Bacterial strains and plasmids.

The *Y. pseudotuberculosis* Yptb1(pYA5199) strains used in this study (17) were grown in Luria Bertani (LB) broth or LB agar plates at 28 °C. Virulent *Y. pestis* KIM6+(pCD1Ap), referred to as *Y. pestis*, was used for challenge studies as previously reported (18). *Y. pestis* were grown in heart infusion broth (HIB) or on HIB plus Congo red agar plates at 28 °C (19). HIB-Congo red agar plates were used to confirm the pigmentation (Pgm^+) phenotype of the *Y. pestis* pathogenic strain (20).

Animal study.

All animal procedures were approved by the Institutional Animal Care and Use Committee (ACUP# 20-01001) at Albany Medical College. Male and female outbred Swiss Webster mice aged 6-8 weeks were procured from Charles River and acclimatized for one week before experiments. For animal immunization, an overnight Yptb1(pYA5199) culture was freshly inoculated in LB broth and incubated at 28 °C with constant agitation (180 rpm) until reaching the exponential growth phase ($OD_{600\ nm}$ = 0.8). Exponentially growing bacterial cells were collected by centrifugation and diluted to the appropriate concentration using sterile 1× phosphate-buffered saline (PBS, pH 7.4). Mice deprived of food and water for 6 h were orally administered a single dose of 5×10^8 CFU (colony-forming units) of Yptb1(pYA5199) in a 200 μl bacterial suspension. Control mice were given an equal volume of sterile PBS. For the pneumonic challenge, mice anesthetized with a ketamine/xylazine mixed solution were infected via the intranasal (i.n.) route with $1\sim5\times10^3$ CFU (10~50 LD_{50}) of *Y. pestis* resuspended in 40 μl of sterile PBS. Animal morbidity and mortality were recorded daily for 15 days. The bacterial burden in different organs of infected mice was determined as described previously (16).

Collection of serum, bronchoalveolar lavage (BAL), and tissue homogenates.

Serum, BAL, and tissue homogenates were collected from mice as described previously (16). The collected cell-free BAL fluid and tissue homogenates were stored at −20 °C until further analysis.

Antibody responses.

Antigen-specific serum IgG, its isotype, or BAL-secreted IgA antibody titers were measured by enzyme-linked immunosorbent assay (ELISA). The antigen-specific [*Y. pestis* cell lysate (YPL), recombinant LcrV (rLcrV), or rF1] antibody titers and isotype profiling were performed as described previously (16).

Western blot analysis.

The Western blot analysis of *Y. pseudotuberculosis* PB1+ and vaccine strain Yptb1(pYA5199) was performed as described previously (16). An LcrV-specific polyclonal antibody was used to analyze both LcrV and $YopE_{Nt138}$-LcrV fusion protein synthesis as well as secretion (21), whereas, an anti-F1 monoclonal antibody (Santa Cruz Biotechnology, CA) was used to detect F1 synthesis.

Antibody transfer, T-cell depletion, and cytokine neutralization.

Eight-week-old naïve Swiss Webster mice were intraperitoneally (i.p.) injected with 50, 100, 250, or 500 μl of serum collected from immunized mice at 28 days post-vaccination (dpv). Naïve mice that received 500 μl of serum from unimmunized mice (sham mice) were considered controls. At 24 h post-administration, mice were i.n. challenged with a 10 LD_{50} lethal dose of *Y. pestis*.

All monoclonal antibodies (mAbs) were supplied by Bio X Cell (West Lebanon, NH). T cells were depleted by i.p. injection with 500 μg of anti-mouse CD4 (clone GK1.5) and/or CD8 (clone 2.43) mAbs initiated 1 day before infection and every other day thereafter. For the localized neutralization of lung $CD4^+$ and/or $CD8^+$ T cells, 200 μg of anti-CD4 (clone GK1.5) and/or anti-CD8 (clone 2.43) mAbs were i.n. injected in 50 μl per mouse. Control mice received an equal quantity of isotype-matched rat IgG2b mAb (clone LTF-2). Cytokines were neutralized by i.p. administration of 200 μg of rat IgG1 mAb specific for IFN-γ (clone XMG1.2) and/or 200 μg of mAb specific for IL-17A (clone 17F3) to each mouse. Control mice received 200 μg of isotype-matched rat IgG1 mAb (clone HRPN).

FTY720 treatment.

To block circulating T cells, mice were fed FTY720 (Santa Cruz Biotechnology, TX, USA) in drinking water at a dose of 0.3 mg/kg/day (9, 22) for 10 days before experiments and maintained until the termination of experiments. Mice provided regular drinking water served as controls.

Isolation of lung cells, T-cell sorting, and adoptive transfer.

The lungs from euthanized mice were perfused with 50 ml of sterile PBS by heart aortic injection twice, removed aseptically, and then chopped and digested with a Liberase™ TL (1 mg/ml; Roche) and DNase I (10 mg/ml; Sigma) cocktail for 30 min at 37 °C with gentle agitation. Then, the digested lungs were dissociated using 70-μm strainers to obtain single cells, followed by red blood cell (RBC) lysis. Lung T_{RM} cells were differentiated from circulating T cells by intravenous (i.v.) administration with 5 μg of FITC-conjugated anti-CD45.2 mAbs diluted in 200 μl of sterile PBS via the tail vein. Five minutes post-injection, the mice were euthanized, and lung single cells were isolated as described previously (23).

Lung $CD4^+$ and/or $CD8^+$ T cells were purified using T-cell isolation kits (MojoSort Nanobeads, BioLegend) according to the manufacturer's protocol. At 24 h post-irradiation (5 Gray), naïve mice were intravenously injected with 2×10^6 cells/mouse via the tail vein. Naïve mice that received an equal number of lung T cells from sham mice were considered controls. FACS sorting was performed using a FACSAria II (BD) three-laser sorter. To sort lung T_{RM} and circulating T cells, lung single cells were isolated from immunized and sham mice with i.v. injection of FITC-conjugated anti-CD45.2 mAbs as described above. Lung $CD4^+$ and/or $CD8^+$ T cells were purified using T-cell isolation kits (MojoSort Nanobeads, BioLegend) according to the manufacturer's protocol. Purified lung T cells from five mice of the same group were pooled into each sample, and $CD45^+$ and $CD45^-$ T cells were further separated by FACS sorting. Then, sorted lung T_{RM} and circulating T cells (2×10^5) in 50 μL of sterile PBS were injected individually into irradiated naïve mice by

the intratracheal route. On Day 1 post-cell transfer, the recipient mice were intranasally challenged with 10 LD_{50} of *Y. pestis*. Animal survival was recorded for 15 days (16).

Analysis of *in vitro* and *in vivo* T-cell or T_{RM} activation.

To determine *in vitro* activation, lung single cells (2×10^6) were seeded in 12-well cell culture plates and stimulated for 72 h with 20 μg/ml of YPL, purified endotoxin-free LcrV or F1. Two hours before collection, culture media were supplemented with a 1× brefeldin-A and monensin cocktail (1:1 ratio) to block Golgi-mediated cytokine secretion. To determine *in vivo* activation, lung cells (2×10^6) isolated from pulmonary *Y. pestis*-infected mice were induced by 50 ng/mL phorbol myristate acetate (PMA) and 1 μg/mL ionomycin for 1 h and then treated with the 1× brefeldin-A and monensin cocktail for another 2 h (24). Each T-cell culture was routinely performed in triplicate. Induced cells were harvested and resuspended in Flow Cytometry Staining (FACS) buffer containing Fc block (anti-mouse CD16/32 antibodies) (1:200) for 10 min on ice. T cells and their cytokine production were analyzed using FACS.

To examine whether lung resident ($CD45^-$) cells are responsive to the specific *Y. pestis* antigen, the $CD45^-$ $CD4^+$ or $CD45^-$ $CD8^+$ cells sorted out from lungs of Yptb1(pYA5199) immunized and sham mice were induced with LcrV-pulsed lung dendritic cells for 48 h. Two hours before the collection of cells, culture media were supplemented with a 1× brefeldin-A and monensin cocktail (1:1 ratio). *In vitro* stimulated lung $CD4^+$ or $CD8^+$ T_{RM} cells were FACS analyzed by following staining and acquisition procedures consistent with T cells.

Flow cytometry.

All cells were stained with dead/live Zombie-Red following labeling with the appropriate antibodies in FACS buffer. T lymphocytes were stained for CD3, PECy7 or APCCy7 (clone 145-2C11), CD4, PE (clone GK1.5), CD8, APC (clone 53-6.7), CD44, BV650 (clone IM7), CD69, PerCPCy5.5 (clone H1.2F3), CD103, PECy7 (clone 2E7), and CD62L, HV510 (clone MEL-14) depending on the experiment, followed by fixation and permeabilization by using BD Biosciences Perm-Fix Solution. To detect cytokines, permeabilized cells were stained for IFN-γ, BV785 (clone XMG1.2), TNF-α, BV510 (clone MP6-XT22), and IL-17A, APCCy7 (clone TC11-18H10.1) for 1 h on ice. Myeloid cells from the lung single-cell and BAL isolations were stained with dead/live (Zombie-Red) and for surface CD45, FITC (clone QA17A26), CD11b, BV510 (clone M1/70), CD11c, APCCy7 (clone N418), Ly6G, PECy7 (clone IA8), F4/80, Pacific Blue (clone BM8), and Siglec-F, APC (clone S17007L). Fluorescently labeled antibodies were purchased from BD Biosciences and BioLegend. Flow cytometry was performed using a BD FACSymphony™ A3 (BD Biosciences) with FACS Diva software and analyzed using FlowJo v10.8.

Statistical analysis.

All statistical calculations were performed using GraphPad Prism 9.0. Statistical analysis between the two groups was performed by using an unpaired t-test and a two-tailed Mann–Whitney U test. Tests among multiple groups were performed using one-way or two-way ANOVA with Tukey's test for multiple comparisons. Survival curves were evaluated by the log-rank Mantel-Cox test, and weight loss data were analyzed by using a two-tailed Mann–

Whitney U test. Data are presented as the mean value ± standard deviation with significance indicated by ns, no significance, * $p< 0.05$; **, $p< 0.01$; ***, $p<0.001$; or ****, $p< 0.0001$.

Results

Oral Yptb1(pYA5199) vaccination confers substantial protection against pulmonary *Y. pestis* challenge.

The plague vaccine candidate, Yptb1(pYA5199), simultaneously delivered the *Y. pestis* protective antigens LcrV and F1 (Fig. S1A). A single-dose oral administration of 5×10^8 CFU of Yptb1(pYA5199) afforded 83% protection against pulmonary infection via i.n. challenge with 5×10^3 CFU (50 LD_{50}) of *Y. pestis*. All sham mice succumbed within 4 days after the same challenge (Fig. 1A). The *Y. pestis* titers in the lung, spleen, and liver of Yptb1(pYA5199)-immunized mice were substantially lower at 2 days post-infection (dpi) than those of sham mice (Fig. 1B). No *Y. pestis* was recovered from those organs at 4 dpi in the Yptb1(pYA5199)-immunized mice (data not shown).

Single-dose oral Yptb1(pYA5199) vaccination induced the production of high serum IgG titers to YPL on day 14, with a substantial increase on day 28. Both the IgG2a/IgG1 and IgG2b/IgG1 ratios were close to 1, indicating the induction of balanced Th1/Th2 responses (Fig. 1C). Yptb1(pYA5199) vaccination also primed strong LcrV- and F1-specific antibody titers with balanced isotype profiles (Fig. S1B). Lung $CD4^+$/$CD8^+$ T cells *in vitro* stimulated with either YPL, LcrV, or F1 for 72h were determined by flow-cytometric analysis (Fig. 1D and S1C). Results showed that the number of both lung $CD4^+$ and $CD8^+$ T cells from Yptb1(pYA5199)-immunized mice was substantially higher than that from sham mice after YPL (Fig. 1E), LcrV, or F1 stimulation (Fig. S1D), respectively. Moreover, corresponding lung $CD4^+$ or $CD8^+$ T cells from Yptb1(pYA5199)-immunized mice generated higher IFN-γ, IL-17A, or TNF-α levels than those from sham mice (Fig. 1F) after YPL stimulation.

To further determine whether the protection against pneumonic plague was mediated by antibodies or T cells, immune sera collected from Yptb1(pYA5199)-vaccinated mice were adoptively transferred to naïve mice. Intraperitoneal (i.p.) injection with 500 μl of sera from immunized mice provided partial protection against pulmonary infection with 10 LD_{50} of *Y. pestis*, whereas administration with fewer volumes of the same sera or 500 μl of sera from sham mice failed to offer effective protection (Fig. 1G). The titers of serum anti-YPL antibodies were stable and persistent in surviving recipient mice (Fig. S1E). The i.v. injection of either lung $CD4^+$ or $CD8^+$ T cells provided minimal protection (10-20% survival) for the recipient mice against infection with 10 LD_{50} of *Y. pestis*, whereas transfer of both lung $CD4^+$ and $CD8^+$ T cells offered 80% protection against the same challenge (Fig. 1H). Naïve mice that received both spleen $CD4^+$ and $CD8^+$ T cells from Yptb1(pYA5199)-immunized mice also exhibited 60% survival, whereas naïve mice that received lung or spleen T cells from sham mice failed to survive the same challenge (Figs. 1H and S1F). Moreover, depletion of either $CD4^+$ or $CD8^+$ T cells in Yptb1(pYA5199)-immunized mice moderately diminished protection (anti-$CD4^+$, 55% survival and anti-$CD8^+$, 60% survival) against pulmonary infection with 50 LD_{50} of *Y. pestis*, while depletion of both $CD4^+$ and $CD8^+$ T cells significantly reduced protection (33% survival) compared to the administration of isotype control antibodies (Figs. 1I and

S1G). Collectively, our data signified that lung $CD4^+$ and $CD8^+$ T cells elicited by oral Yptb1(pYA5199) vaccination played a dominant role in controlling pulmonary *Y. pestis* infection and that primed *Y. pestis*- and its antigen-specific antibodies partially conferred dose-dependent protection.

Lung-resident T (T_{RM}) cells established by oral Yptb1(pYA5199) vaccination are highly activated upon pulmonary *Y. pestis* infection.

Experienced lung T_{RM} cells after infection or immunization can rapidly respond to homologous and heterologous infections and facilitate pathogen clearance in the lung mucosal site (9, 10, 25). Therefore, we sought to determine the composition of lung-infiltrating memory T cells in Yptb1(pYA5199)-vaccinated mice. To do so, FITC-conjugated mouse anti-CD45.2 antibodies were intravenously injected to label circulating lymphocytes but not tissue-bound lymphocytes as described previously (23) (9, 26). Memory T cells, such as T_{CM} ($CD44^{lo}$ $CD62L^{hi}$ $CD69^{lo}$), T_{EM} ($CD44^{hi}$ $CD62L^{lo/-}$ $CD69^{lo}$), or T_{RM} ($CD44^{hi}$ $CD62L^{lo}$ $CD69^{hi}$ $CD103^{+/-}$) cells, can be differentiated based on CD44, CD62L, CD69, and/or CD103 surface markers (9, 23), as gated in Fig. S2A. At 42 dpv, the absolute number of lung $CD4^+$ and $CD8^+$ T_{RM} cells gated with $CD45^-$ $CD44^+$ $CD62L^-$ $CD69^+$ markers in Yptb1(pYA5199)-immunized mice increased approximately 25-fold compared to that in sham mice upon *in vitro* stimulation by PMA and ionomycin. The number of $CD4^+$ T_{RM} cells producing IFN-γ, TNF-α, and/or IL-17A was substantially higher than that in sham mice (Figs. 2A, and S2B). Moreover, ~8-10% of lung $CD4^+$ T_{RM} cells from Yptb1(pYA5199)-immunized mice were either IL-$17A^+$ IFN-γ^+ or IL-$17A^+$ TNF-α^+ double-positive cells, whereas the percentage of those respective cells in sham mice was negligible (Fig. 2A). Similarly, the number of lung $CD8^+$ T_{RM} cells producing IFN-γ, TNF-α, and/or IL-17A were substantially higher (6-15 folds) in Yptb1(pYA5199)-immunized mice than that in sham mice (Fig. 2A and S2B). The number of IL-$17A^+$ IFN-γ^+ but not IL-$17A^+$ TNF-α^+ double-positive $CD8^+$ T_{RM} cells from Yptb1(pYA5199)-immunized mice was substantially higher than that from sham mice, but the number of both double-positive $CD8^+$ T_{RM} cells was relatively low in comparison to the respective number of lung $CD4^+$ T_{RM} cells (Fig. 2A).

Next, we investigated the activation of lung T_{RM} cells during pulmonary *Y. pestis* infection. At 2 dpi, lung $CD4^+$ T_{RM} cells and those cells producing IL-17A, IFN-γ, or TNF-α in Yptb1(pYA5199)-immunized mice showed 3-4-fold increases in counts compared to those in Yptb1(pYA5199)-immunized mice without infection, respectively (Figs. 2A&2B and S2B&S2C). The numbers of the respective lung $CD4^+$ T_{RM} cells in post-infected sham mice showed a 2-3 fold increase in comparison to those in pre-infected sham mice but were substantially lower than those in Yptb1(pYA5199)-immunized mice at 2 dpi (Figs. 2A&B and S2B&S2C). Additionally, a substantial proportion of (40-60%) the $CD4^+$ T_{RM} cells ($CD44^+$ $CD69^+$) produced IL-17A after infection (Fig. 2B). Among IL-$17A^+$ $CD4^+$ T_{RM} cells, ~55% of the cells coproduced IFN-γ or TNF-α. In addition, the counts of lung $CD8^+$ T_{RM} cells and those cells producing either IFN-γ or TNF-α in post-infected Yptb1(pYA5199)-immunized mice were increased 2-4-fold compared to those in pre-infected Yptb1(pYA5199)-immunized mice (Figs. 2A&B and S2B&S2C). In contrast to the number of $CD4^+$ T_{RM} cells, the number of IL-$17A^+$ $CD8^+$ T_{RM} cells in

Yptb1(pYA5199)-immunized mice at 2 dpi producing either IFN-γ or TNF-α was slightly higher than that in sham mice, but the difference was not significant (Fig. 2B).

CD103, as a cell marker, is usually considered to be expressed by certain subsets of $CD8^+$ T_{RM} cells and not significantly by $CD4^+$ T_{RM} cells (8, 27). However, we found that approximately 8-9% of $CD45^-$ lung CD4 and CD8 T_{RM} cells in Yptb1(pYA5199)-immunized mice retained the $CD103^+$ marker, and the number of lung $CD103^+$ $CD4^+$ T_{RM} cells in immunized mice was ~35-fold higher than that in sham mice (Fig. S2D). The number of lung $CD103^+$ $CD8^+$ T_{RM} cells in Yptb1(pYA5199)-immunized mice was 12-fold higher than that in sham mice (Fig. S2D). Next, we examined lung $CD4^+$ and $CD8^+$ T_{RM} cells expressing $CD103^+$ during *Y. pestis* infection. At 2 dpi, a 4-fold increase in the number of lung $CD4^+$ T_{RM} cells expressing $CD103^+$ was observed in comparison to that in pre-infected Yptb1(pYA5199)-immunized mice, while no substantial increase in the number of lung $CD8^+$ $CD103^+$ T_{RM} cells (Fig. S2D and E). Furthermore, kinetic analysis of lung $CD69^+$ $CD4^+$ and $CD69^+$ $CD8^+$ T_{RM} cells was performed from 1 to 6 dpi. The number of lung $CD4^+$ T_{RM} cells progressively increased from 1 to 4 dpi and reached a plateau at 6 dpi (Fig. 2C). However, the number of lung $CD8^+$ T_{RM} cells continued to increase from 1 to 2 dpi and remained constant from 2 to 6 dpi (Fig. 2C). Overall, both different subsets of $CD4^+$ and $CD8^+$ T_{RM} cells were established at the lung mucosal site of Yptb1(pYA5199)-immunized mice and substantial increase in the number of both lung $CD4^+$ and $CD8^+$ T_{RM} cells post pulmonary *Y. pestis* infection, suggesting that they might have important roles in protection against pneumonic plague.

T_{RM} cells residing in the lungs of Yptb1(pYA5199)-immunized mice offer protection against pulmonary *Y. pestis* infection.

FTY720 treatment blocks the egress of lymphocytes from lymph nodes or secondary lymphoid organs to peripheral blood and prevents infiltration of lymphocytes to nonlymphoid organs, including the lungs (9, 22). To examine the protective role of lung T_{RM} cells, circulating T cells were blocked in mice by oral feeding with FTY720 for 10 days before infection and during the entire course of infection (Fig. 3A). The populations of $CD3^+$, $CD4^+$, and $CD8^+$ T cells in the lungs, spleen, and blood of FTY720-treated mice were quantified by flow cytometry. The results showed that T lymphocytes in the blood of representative mice were almost completely blocked (Fig. S3A). The FTY720 treatment led to a 20- and 50-fold reduction in the counts of lung T_{CM} cells ($CD62L^+$) of FTY720-treated Yptb1(pYA5199)-immunized mice (termed Yptb1(pYA5199)+FTY720 mice) compared with those in sham and Yptb1(pYA5199)-immunized mice, respectively, but did not significantly reduce the number of $CD4^+$ and $CD8^+$ T_{CM} cells in the spleens (Fig. S3B). Additionally, treatment with or without FTY720 did not impair the potent humoral and splenic T-cell immune responses in Yptb1(pYA5199)-immunized mice (Figs. S3C-D). Before *Y. pestis* challenge, FTY720 treatment increased the number of lung $CD4^+$ T_{RM} cells and those cells producing IFN-γ, TNF-α, and/or IL-17A to different extents compared to that with nontreatment of Yptb1(pYA5199)-immunized mice (Figs. 2A, 3B, S2B, and S3E). The number of respective cells was further elevated in immunized mice both with or without FTY720 treatment post-*Y. pestis* challenge (Figs. 2B, 3C, S2C, and S3F). However, the increased proportions of these respective cells in Yptb1(pYA5199)-immunized

mice before and after the challenge were comparable to those in Yptb1(pYA5199)+FTY720 mice. In addition, the number of lung $CD8^+$ T_{RM} cells and those cells producing IFN-γ, TNF-α, and/or IL-17A in Yptb1(pYA5199)+FTY720 mice were comparable to those in Yptb1(pYA5199)-immunized mice before or after *Y. pestis* infection (Figs. 2A-B, 3B-C, S2B&C, and S3E-F).

Although Yptb1(pYA5199)+FTY720 mice manifested a significant decrease in the number of lung T_{CM} cells (Fig. S3B), those mice still demonstrated the same protection against pulmonary challenge with 50 LD_{50} of *Y. pestis* (Fig. 3D) and similar *Y. pestis* burden in organs (Fig. 3E) to the Yptb1(pYA5199)-immunized mice (Fig. 1A and B). Additionally, we treated mice with FTY720 for 10 days to eliminate circulatory T cells before immunization and thereafter for the entire experiment (Fig. 3F). The treated mice were designated pre-FTY720-Yptb1(pYA5199) mice. At 42 dpv, the number of lung $CD4^+$ and $CD8^+$ T_{RM} cells in pre-FTY720-Yptb1(pYA5199) mice was comparable to that in Yptb1(pYA5199)+FTY720 mice (Fig. 3G). In Yptb1(pYA5199)-immunized animals, FTY720 pretreatment slightly reduced the protection (60% survival) against pneumonic plague challenge, which presented no significant difference in comparison to without FTY720 or with FTY720 posttreatment (Fig. 3H).

Furthermore, lung circulating T cells (referred to $CD45^+$) and T_{RM} cells (referred to $CD45^-$ cells) were sorted from sham and Yptb1(pYA5199)-immunized mice intravenously injected with FITC-conjugated anti-CD45.2 mAbs. To check the antigen specificity in lung T_{RM}, $CD45^-$ cells were *in vitro* stimulated with the recombinant LcrV protein pulsed dendritic cells and were assessed for the expression of IFN-γ, TNF-α, and/or IL-17A. Consistent with the pre-infection T_{RM} data obtained from Yptb1(pYA5199) and Yptb1(pYA5199)+FTY720 (Figs 2A and 3B, respectively), the number of IL-$17A^+$ $CD4^+$ T_{RM} cells in Yptb1(pYA5199)-immunized mice were increased around 45 fold compared to sham (Fig S3G). The majority (40-50%) of IL-$17A^+$ $CD4^+$ T_{RM} were coexpressed with IFN-γ or TNF-α. However, $CD8^+$ T_{RM} in Yptb1(pYA5199)-immunized mice were predominantly expressing IFN-γ or TNF-α (Fig S3G). Naïve mice that intratracheally received both sorted $CD45^-$ lung $CD4^+$ and $CD8^+$ T_{RM} cells from Yptb1(pYA5199)-immunized mice exhibited 50% survival upon challenge with 10 LD_{50} of *Y. pestis*, while mice that received respective lung $CD4^+$ and $CD8^+$ T cells from circulating ($CD45^+$) lineage showed very marginal survival (Fig. 3I). Naïve mice that received the individual population of lung T cells from immunized mice failed to survive the same challenge (Fig. 3I). All naïve mice received intratracheally injection with sham $CD45^-$ or $CD45^+$ $CD4^+$ and $CD8^+$ together or individually were succumbed to death by 4 dpi against the similar dose of *Y. pestis* challenge (Fig S3H). Our results suggested that local induction of lung $CD4^+$ and $CD8^+$ T_{RM} in oral Yptb1(pYA5199)-immunized mice acted as a first line of protection against pulmonary *Y. pestis* infection.

Lung $CD4^+$ and $CD8^+$ T_{RM} cells counteract pulmonary *Y. pestis* infection.

Furthermore, we locally depleted lung T cells in Yptb(pYA5199)+FTY720 mice by intranasally administering anti-CD4,-CD8 mAbs, or both (Fig. 4A) and found that lung T-cell populations but not spleen T-cell populations were significantly reduced (S4A). In

comparison to the isotype control, the treatments that locally depleted either lung $CD4^+$ T cells alone or $CD4^+$ and $CD8^+$ T cells both significantly diminished survival (40% survival) of the Yptb1(pYA5199)+FTY720 mice against pulmonary challenge with 10 LD_{50} of *Y. pestis*, whereas lung $CD8^+$ T-cell depletion alone moderately reduced survival (60%) (Fig. 4B). At 2 dpi, *Y. pestis* titers in the lung showed a 2-3 $\log_{10}$-fold increase in the Yptb1(pYA5199)+FTY720 mice with local depletion of $CD4^+$ T cells alone or $CD4^+$ and $CD8^+$ T cells both and an ~1 $\log_{10}$-fold increase with local depletion of $CD8^+$ T cells compared with those with the isotype control (Fig. 4C).

The hallmark of primary pneumonic plague in naïve mice after 48 h of exposure is that the BAL fluid and lung manifest highly increased neutrophil counts and dramatically decreased alveolar macrophage (AM) counts (1). Therefore, we sought to examine the effect of local lung T-cell depletion on neutrophil and AM counts (Fig. S4B) in the lungs and cytokine production at 2 dpi. In the lung and BAL fluid, the frequency and number of neutrophils ($CD11b^+$ $Ly6G^+$, Fig. S4C) substantially increased in the Yptb1(pYA5199)+FTY720 mice locally depleted for both $CD4^+$ and $CD8^+$ T cells and slightly increased in mice depleted for either $CD4^+$ or $CD8^+$ T cells compared to those in the isotype-treated mice but were still significantly lower than those in *Y. pestis*-infected sham mice (Figs. 4D&E and S4C&D). In contrast, a substantial reduction in the frequency and number of AMs ($CD11b^{hi}$ $CD11c^{hi}$ $F4/80^{hi}$ Siglec F^{hi}, Fig. S4B) in the lung and BAL was observed in the Yptb1(pYA5199)+FTY720 mice locally depleted for $CD4^+$, $CD8^+$, or both T cells compared with those in the isotype-treated mice (Figs. 4D&F and S4C&E). The frequency and number of AMs in the BAL fluid and lung of Yptb1(pYA5199)+FTY720 mice depleted for either $CD4^+$ or $CD8^+$ T cells were still higher than those of *Y. pestis*-infected sham mice (Figs. 4F and S4E). Consistent with previous studies (28, 29), sham mice produced high levels of IL-1β in the BAL fluid at 2 dpi, whereas Yptb1(pYA5199)+FTY720 mice treated with isotype antibodies had minimal levels of IL-1β in the BAL fluid that were comparable to those in the BAL fluid of noninfected naïve mice (Fig. 4G). Levels of IL-1β in the BAL fluid were significantly increased in the Yptb1(pYA5199)+FTY720 mice depleted for $CD4^+$, $CD8^+$, or both T cells compared to those in the isotype-treated mice but were comparable to those in sham mice (Fig. 4G). The patterns in the levels of chemokines such as granulocyte colony-stimulating factor (G-CSF) and keratinocyte cell-derived chemokine (KC) were similar to those in the levels of IL-1β (Fig. 4G), which were associated with high recruitment of lung neutrophils during infection (29). Consistent with the above results, the levels of IL-17A in the BAL fluid of Yptb1(pYA5199)+FTY720 mice treated with isotype antibodies at 2 dpi were substantially higher than those in mice depleted for $CD4^+$, $CD8^+$, or both T cells or in sham mice (Fig. 4G). The low levels of IL-17A in the BAL fluid were comparable among Yptb1(pYA5199)+FTY720 mice depleted for $CD4^+$, $CD8^+$, or both T cells, sham mice, and naïve mice (Fig. 4G). The patterns of IFN-γ were similar to those of IL-17A (Fig. 4G). Thus, our results suggest that lung $CD4^+$ and $CD8^+$ T_{RM} cells primed by oral Yptb1(pYA5199) immunization are required to orchestrate other lung immune cells during pulmonary *Y. pestis* infection.

The synergistic role of IFN-γ and IL-17A promotes protective immunity against pneumonic plague.

Previous findings have shown the synergistic role of Th1- and Th17-mediated host immune responses against extracellular or intracellular pathogens, including *Y. pestis* (13, 14). The elicited Th17 memory cells at the lung mucosal site promote Th1-mediated long-term protection against bacterial pathogens (30). Our results revealed that lung $CD4^+$ T_{RM} cells from Yptb1(pYA5199)-immunized mice consistently produced significant amounts of IL-17A and/or IFN-γ upon restimulation *in vitro* and *in vivo* (Figs 2A&B, S2B&C, and S3H). Therefore, we further examined the protective and regulatory roles of these cytokines against pneumonic plague. In Yptb1(pYA5199)-immunized mice, IFN-γ neutralization slightly reduced the protective efficacy (70% survival), and IL-17A neutralization moderately reduced protection (55% survival) against pulmonary infection with 50 LD_{50} of *Y. pestis* in comparison to that with the isotype IgG control (80% survival), while concurrent neutralization of IL-17A and IFN-γ led to marginal protection (15% survival) against the same challenge (Figs. 5A and B). At 2 dpi, the lung *Y. pestis* burden in each group of mice reflected animal survival to a large extent. *Y. pestis* CFU in the lungs of Yptb1(pYA5199)-immunized mice treated with anti-IFN-γ antibodies alone were comparable, while those of mice treated with anti-IL-17A antibodies alone were significantly increased compared to those of mice treated with the isotype control (Fig. 5C). Bacterial CFU in the lungs of Yptb1(pYA5199)-immunized mice that received both anti-IL-17A and anti-IFN-γ mAbs were comparable to those of sham mice but were significantly higher than those of Yptb1(pYA5199)-immunized mice treated with the isotype control, anti-IFN-γ, or anti-IL-17A antibodies alone (Fig. 5C).

A previous report showed that IL-17-synthesizing neutrophils coordinating with IFN-γ-activated macrophages conferred protection against pneumonic plague (31). Thus, we examined neutrophils and AMs in the BAL fluid and lungs of IL-17A-, IFN-γ-, or both IFN-γ/IL-17A-neutralized mice after *Y. pestis* infection. At 2 dpi, sham mice displayed a high number of neutrophils and a low number of AMs in the lungs and BAL fluid, while Yptb1(pYA5199)-immunized mice treated with the isotype IgG displayed a dramatically low number of neutrophils but a high number of AMs (Figs. 5D-G), which was consistent with previous results (Figs. 4E&F and S4D&E). In comparison to the isotype control, anti-IFN-γ treatment alone resulted in a 3-4-fold increase in BAL fluid and lung neutrophil counts but a 2.5-4-fold decrease in BAL fluid and lung AM counts, whereas anti-IL-17A treatment alone resulted in a 3-4-fold decrease in the number of AMs and a comparable number of neutrophils in the lung and BAL fluid samples of immunized mice, respectively (Figs. 5D-G). Neutralization of both IFN-γ and IL-17A led to a ~4-fold increase in neutrophil counts in the BAL fluid and lung and a 5-6-fold reduction in AM counts in the BAL fluid and lung compared to those with the isotype control (Figs. 5D, E, F, and G). Additionally, compared to the isotype control, neutralization of IL-17A, IFN-γ, or both substantially reduced the numbers of lung $CD4^+$ and $CD8^+$ T_{RM} cells to different extents (Figs. 5H and I).

Moreover, cytokines and chemokines in the BAL fluid of the respective mice at 2 dpi were analyzed. In comparison to the isotype control in Yptb1(pYA5199)-immunized mice, neutralization of IL-17A alone or both IL-17A and IFN-γ led to a 2-3-fold increase in IL-1β

production, while neutralization of IFN-γ alone did not. The levels of IL-1β in the BAL fluid of immunized mice treated with anti-IFN-γ antibodies were comparable to those of sham mice (Fig. 5J). The patterns of IL-1β were similar to those of G-CSF and KC in the BAL fluid of the respective mice (Fig. 5J). Compared with those with the isotype control, the levels of IL-17A in the BAL fluid were dramatically reduced by anti-IL-17A treatment alone or both anti-IL-17A and anti-IFN-γ treatment but not by anti-IFN-γ treatment alone. The levels of IFN-γ in the BAL fluid of mice treated with anti-IL-17A or anti-IFN-γ antibodies alone or both were comparable to those of sham mice but significantly lower than those of isotype IgG-treated mice (Fig. 5J). Compared to those in sham mice at 2 dpi (Fig. 5K), lung histopathologic signatures in Yptb1(pYA5199)-immunized mice with both IL-17A and IFN-γ neutralization displayed severe lung lesions, hemorrhage, reduced alveolar lacunar space, and epithelial desquamation, whereas mice treated with either anti-IL17 or anti-IFN-γ antibodies showed moderate lung inflammation and hemorrhage. The isotype control-treated mice showed normal lung architecture after *Y. pestis* infection, without significant lesions (Fig. 5K). Our results suggest that both IFN-γ and IL-17A play pivotal roles in the coordination of lung T_{RM} cells, neutrophils, and AMs during *Y. pestis* infection.

Lung T_{RM} cells confer long-term protection against intranasal *Y. pestis* infection.

Next, we monitored antibody and T-cell responses in Yptb1(pYA5199)-immunized mice with or without FTY720 treatment for 120 dpv and in the course of pulmonary *Y. pestis* challenge (Fig. 6A). A single-dose oral Yptb1(pYA5199) vaccination stimulated the production of persistent anti-YPL IgG titers in mice that were maintained until 90 dpv and moderately declined at 120 dpv. Continuous treatment with FTY720 from day 20 to day 120 had no significant impact on serum antibody titers compared to those with non-FTY720 treatment (Fig. S4F). In addition, long-term FTY720 treatment led to the blockage of circulating T-cell infiltration into the lung and reduced lung YPL-specific T-cell counts in Yptb1(pYA5199)-immunized mice compared to those with non-FTY720 treatment (Figs. S4G-H).

Furthermore, the kinetics of lung $CD4^+$ and $CD8^+$ T_{RM} cells were examined in the course of immunization. Consistent with previous studies (30, 32, 33), our results showed that those cells in immunized mice both with or without FTY720 treatment were substantially higher than those in sham mice, and lung T_{RM} cells maintained significant levels from 30 dpv until 120 dpv (Fig. 6B). Similar numbers of lung $CD4^+$ T_{RM} cells were established in the lungs of Yptb1(pYA5199)-vaccinated mice with or without FTY720 treatment at different time points. However, the number of $CD8^+$ T_{RM} cells in Yptb1(pYA5199)+FTY720 mice was substantially higher than that in sham mice but significantly less than that in Yptb1(pYA5199)-immunized mice at different time points (Fig. 6B). At 2 dpi, both Yptb1(pYA5199)-vaccinated mice with or without long-term FTY720 treatment displayed rapid proliferation of lung $CD4^+$ and $CD8^+$ T_{RM} cells compared to that of sham mice (Fig. 6C). The number of lung $CD4^+$ T_{RM} cells in long-term FTY720-treated Yptb1(pYA5199)-immunized mice slightly increased in comparison to that in Yptb1(pYA5199)-immunized mice, but the difference was not significant, while the number of lung $CD8^+$ T_{RM} cells in Yptb1(pYA5199)+FTY720 mice was substantially higher than that in Yptb1(pYA5199)-

immunized mice (Fig. 6C). The number of lung $CD4^+$ T_{RM} cells producing IFN-γ, TNF-α, and/or IL-17A was similar in both FTY720-treated and untreated Yptb1(pYA5199)-immunized mice but was dramatically higher than that in sham mice at 2 dpi (Figs. 6C).

Challenge studies demonstrated that similar protection against pulmonary *Y. pestis* was maintained between 42 and 120 dpv with a single dose of oral Yptb1(pYA5199) (Figs. 1D and 6D), and long-term FTY720 treatment slightly decreased protection against the same challenge, but the difference was not significant (Fig. 6D). Additionally, *Y. pestis* CFUs in the lungs were comparable in Yptb1(pYA5199)-immunized mice with or without long-term FTY720 treatment but were significantly lower than those in unvaccinated mice (Fig. 6E). Interestingly, long-term FTY720-treated Yptb1(pYA5199)-immunized mice had relatively higher *Y. pestis* counts in the spleen and liver than Yptb1(pYA5199)-immunized mice (Fig. 6E), but *Y. pestis* was cleared from the lung, liver, and spleen of both immunized mice at 4 dpi (data not shown). Collectively, these results suggested that oral Yptb1(pYA5199) vaccination elicited the production of *Y. pestis*-specific lung T_{RM} cells that confer long-lasting protective immunity against pneumonic plague.

Discussion

In general, the induction of both potent humoral and cellular immune responses is an ideal strategy to develop effective plague vaccines (14, 34, 35). *Y. pestis*-specific antibodies induced by immunization can offer protection against pneumonic plague in certain rodent models (36, 37), but antibody-mediated protection is highly variable, as demonstrated in nonhuman primate models (38, 39) and outbred mouse models (40, 41). Oral Yptb1(pYA5199) vaccination stimulated both robust *Y. pestis*-specific antibody and T-cell responses in Swiss Webster mice (Fig. 1). Consistent with previous studies (42, 43), T cells activated by oral Yptb1(pYA5199) immunization made a major contribution to protect against pneumonic plague, and antibodies produced in response to immunization had a collaborative role to a certain extent (Fig. 1). Discrepancies in the roles of *Y. pestis*- or its antigen-specific antibodies against pneumonic plague among previous studies (44-46) are not well examined yet. We speculate that the type of vaccine, immune components included in vaccines, animal genetic variation, immunization routes, and other factors may lead to variable pneumonic plague protection mediated by antibody responses.

T_{RM} cells residing in nonlymphoid tissues (NLTs) lack homing molecular CCR7 and CD62L to secondary lymphoid organs (SLOs) and increase express of CD69, CXCR3, CD49a, and/or CD103 molecular (47, 48). T_{RM} cells have been shown to act as immune sentinels via the rapid production of cytokines and chemokines and facilitate counteracting the secondary pathogen infection (49, 50). Lung cognate antigen recognition can substantially improve the activation of pulmonary T_{RM} cells (9, 32, 51), and vaccines aiming to generate lung T_{RM} cells should deliver antigens into the airways. The Yptb1(pYA5199) vaccine strain could rapidly disseminate to the lung after oral vaccination and persisted in the lung for 2 weeks before complete clearance (Fig. S1D). Therefore, lung T_{RM} cells might be directly stimulated and expanded in situ by APCs presenting *Yersinia* antigens. Studies have revealed that T_{RM} cells in NLTs can undergo stimulation and proliferation in response to local infection (52-54). Consistent with previous studies (9, 30, 32, 51), our results also

demonstrated that lung T_{RM} cells afforded much better defense against *Y. pestis* infection than lung circulating T cells (Fig. 3D and H). Moreover, an intratracheal transfer of 2×10^5 $CD45^-$ T cells rather $CD45^+$ T cells demonstrated protection against pneumonic plague (Fig. 3I). Therefore, targeting lung T_{RM} cells with a vaccine would be an effective strategy for preventing pneumonic plague. In addition, we demonstrated that spleen T cells primed by oral Yptb1(pYA5199) immunization played an important role in protection against pneumonic plague (Fig. S1F), which was consistent with previous studies that documented *Y. pestis*-specific memory T cells in the spleen of mice immunized with different *Y. pestis* vaccines (55, 56). The spleen, as an SLO, has generally been considered a transit site for T_{CM} and T_{EM} cells, but recent studies have demonstrated that small numbers of T_{RM} cells can also be established after exposure to antigen(s) or pathogen(s) (57-60). Thus, a small portion of spleen T_{RM} cells from Yptb1(pYA5199)-vaccinated mice transferred by the i.v. route may reside in lung NLTs of naïve mice and provide some protection against pneumonic plague. However, whether the similar protection can be achieved by an intratracheal transfer of the same number of antigen-specific T cells from the blood or spleen is unknown.

Currently, upregulated expression of adhesion molecules, including CD69, CD103, and others, is frequently used to distinguish memory T cells in tissues (T_{RM}) from circulating T cells (48). Among them, CD103 has been considered to be primarily expressed on $CD8^+$ T_{RM} cells but barely on $CD4^+$ T_{RM} cells (50). Recent studies are challenging this paradigm and have revealed that $CD103^+$ $CD4^+$ T_{RM} cells isolated from human and mouse lungs may have a potential role in protection against a secondary challenge (9, 61-63). Our study also showed that $CD103^+$ $CD4^+$ T_{RM} cells were elicited in the lungs of orally Yptb1(pYA5199)-vaccinated mice (Fig. S2D) and 4-5 fold increase in number after *Y. pestis* challenge (Fig. S2E). However, the precise role of $CD103^+$ $CD4^+$ T_{RM} cells in Yptb1(pYA5199)-vaccinated mice needs to be further examined.

Interferon-gamma (IFN-γ) is secreted largely by activated lymphocytes, such as $CD4^+$ T helper type 1 (Th1) cells, $CD8^+$ T cells, and natural killer (NK) cells (64), and is crucial for activating macrophages and preventing pathogenic neutrophil accumulation in the infected lung (65). Macrophage activation by IFN-γ could significantly mitigate *Y. pestis* infection by preventing the excessive accumulation of neutrophils (31). IL-17A, a signature effector cytokine of Th17 cells, induces the production of proinflammatory cytokines, chemokines, and antimicrobial peptides by multiple cell types in the airway and orchestrates the recruitment of neutrophils and macrophages into the airways to mount successful host defense against pathogens (66). After pulmonary *Y. pestis* infection, activated lung T_{RM} cells producing higher amounts of IL-17A, IFN-γ, and/or TNF-α in Yptb1(pYA5199)-vaccinated mice treated both with and without FTY720 displayed combined Th1 and Th17 immune responses and provided substantial short-term and long-term protection against lethal challenge (Figs. 2, 3, and 6). In particular, we noticed that lung $CD4^+$ T_{RM} cells produced a large amount of IL-17A pre- and post-infection. Neutralization of both IFN-γ and IL-17A not only significantly decreased lung $CD4^+$ and $CD8^+$ T_{RM} cell counts but also led to the imbalanced composition of neutrophils and AMs in the BAL fluid of Yptb1(pYA5199)-vaccinated mice and the production of an excessive amount of IL-1β, KC and G-CSF (Fig. 5D-G), which caused severe lung damage (Fig. 5K) and impaired

lung immune functions (Fig. 5). The similar results were observed for the depletion of both lung $CD4^+$ and $CD8^+$ T cells in Yptb1(pYA5199)-vaccinated mice (Fig. 4 E-G). Our study reinforces the dominant role of lung resident T cells and their corresponding cytokines (IFN-γ and IL-17A) against pulmonary *Y. pestis* infection, which has been documented in other bacterial infections (30, 67-69), and suggests that IFN-γ and IL-17A may have synergistic regulatory roles to orchestrate the crosstalk between lung T_{RM} cells and lung neutrophils/alveolar macrophages during pulmonary *Y. pestis* infection.

In this study, both lung $CD4^+$ and $CD8^+$ T cells were required to confer maximal protection by depletion and adoptive transfer of respective cells (Figs. 1H&I, 3I, and 4B). Among them, lung $CD4^+$ T_{RM} cells provided the main source of IL-17A along with IFN-γ and TNF-α production, while lung $CD8^+$ T_{RM} cells produced more IFN-γ and TNF-α than IL-17A (Figs. 2A&B and 3B&C). However, the defined function of lung $CD8^+$ T_{RM} cells in the protection is unclear thus far. Szaba et al reported that TNF-α and IFN-γ were critical and demonstrated complementary roles in $YopE_{69-77}$-specific $CD8^+$ T cell-mediated protection against pneumonic plague (56). A conclusion they drew was that cytokine production, not cytotoxicity, was essential for $CD8^+$ T cell-mediated control of pneumonic plague (56). Our unpublished data also showed that the TNF-α neutralization in Yptb1(pYA5199)-vaccinated mice significantly diminished the protection against pneumonic plague (data not shown). Based on the above information, we speculate that one of the functions of lung $CD8^+$ T_{RM} cells in Yptb1(pYA5199)-immunized mice may provide an additional source of IFN-γ and TNF-α to promote protection. The defined mechanisms will be investigated further.

In the long-term study, we observed that the number of lung $CD8^+$ T_{RM} cells in Yptb1(pYA5199)+FTY720 mice was substantially higher than that in Yptb1(pYA5199)-immunized mice after *Y. pestis* challenge, while the numbers of lung $CD4^+$ T_{RM} cells in the respective mice were comparable (Fig. 6C). Overall, the identification of lung T_{RM} cells activated by oral Yptb1(pYA5199) vaccination and their robust and long-term protective capacities against pulmonary *Y. pestis* infections will provide insight into a new strategy for developing an effective pneumonic plague vaccine.

Supplementary Material

Refer to Web version on PubMed Central for supplementary material.

Acknowledgments

This work was supported by the National Institutes of Health (NIH) grants R01AI125623 and R21AI139703 to WS.

References

1. Pechous RD, Sivaraman V, Stasulli NM, and Goldman WE. 2016. Pneumonic Plague: The darker side of *Yersinia pestis*. Trends Microbiol 24: 190–197. [PubMed: 26698952]
2. Alderson J, Quastel M, Wilson E, and Bellamy D. 2020. Factors influencing the re-emergence of plague in Madagascar. Emerg Top Life Sci 4: 411–421. [PubMed: 33258957]
3. Inglesby TV, Dennis DT, Henderson DA, Bartlett JG, Ascher MS, Eitzen E, Fine AD, Friedlander AM, Hauer J, Koerner JF, Layton M, McDade J, Osterholm MT, O'Toole T, Parker G, Perl TM,

Russell PK, Schoch-Spana M, Tonat K, and Biodefense WGC. 2000. Plague as a biological weapon - Medical and public health management. Jama-J Am Med Assoc 283: 2281–2290.

4. Sun W, and Singh AK. 2019. Plague vaccine: recent progress and prospects. NPJ Vaccines 4: 11. [PubMed: 30792905]
5. 2018. Efficacy trials of Plague Vaccines: endpoints, trial design, site selection. In WHO Workshop 2018. Efficacy trials of Plague Vaccines: endpoints, trial design, site selection, INSERM, Paris, France.
6. Sallusto F, Lenig D, Forster R, Lipp M, and Lanzavecchia A. 1999. Two subsets of memory T lymphocytes with distinct homing potentials and effector functions. Nature 401: 708–712. [PubMed: 10537110]
7. Woodland DL, and Kohlmeier JE. 2009. Migration, maintenance and recall of memory T cells in peripheral tissues. Nat Rev Immunol 9: 153–161. [PubMed: 19240755]
8. Mueller SN, and Mackay LK. 2016. Tissue-resident memory T cells: local specialists in immune defence. Nat Rev Immunol 16: 79–89. [PubMed: 26688350]
9. Wilk MM, Misiak A, McManus RM, Allen AC, Lynch MA, and Mills KHG. 2017. Lung CD4 tissue-resident memory T cells mediate adaptive immunity induced by previous infection of mice with *Bordetella pertussis*. J Immunol 199: 233–243. [PubMed: 28533445]
10. Wang H, Hoffman C, Yang X, Clapp B, and Pascual DW. 2020. Targeting resident memory T cell immunity culminates in pulmonary and systemic protection against *Brucella* infection. PLoS Pathog 16: e1008176. [PubMed: 31951645]
11. McGill J, and Legge KL. 2009. Cutting Edge: Contribution of lung-resident T cell proliferation to the overall magnitude of the antigen-specific CD8 T cell response in the lungs following murine influenza virus infection. J Immunol 183: 4177–4181. [PubMed: 19767567]
12. Christensen D, Mortensen R, Rosenkrands I, Dietrich J, and Andersen P. 2017. Vaccine-induced Th17 cells are established as resident memory cells in the lung and promote local IgA responses. Mucosal Immunol 10: 260–270. [PubMed: 27049058]
13. Lin JS, Kummer LW, Szaba FM, and Smiley ST. 2011. IL-17 contributes to cell-mediated defense against pulmonary *Yersinia pestis* infection. J Immunol 186: 1675–1684. [PubMed: 21172869]
14. Parent MA, Wilhelm LB, Kummer LW, Szaba FM, Mullarky IK, and Smiley ST. 2006. Gamma interferon, tumor necrosis factor alpha, and nitric oxide synthase 2, key elements of cellular immunity, perform critical protective functions during humoral defense against lethal pulmonary *Yersinia pestis* infection. Infect Immun 74: 3381–3386. [PubMed: 16714568]
15. Szaba FM, Kummer LW, Wilhelm LB, Lin JS, Parent MA, Montminy-Paquette SW, Lien E, Johnson LL, and Smiley ST. 2009. D27-pLpxL, an avirulent strain of *Yersinia pestis*, primes T cells that protect against pneumonic plague. Infect Immun 77: 4295–4304. [PubMed: 19620344]
16. Singh AK, Curtiss R 3rd, and Sun W. 2019. A recombinant attenuated *Yersinia pseudotuberculosis* vaccine delivering a *Y. pestis* YopENt138-LcrV fusion elicits broad protection against plague and yersiniosis in mice. Infect Immun 87.
17. Majumder S, Olson RM, Singh A, Wang X, Li P, Kittana H, Anderson PE, Anderson DM, and Sun W. 2022. Protection induced by oral vaccination with a recombinant *Yersinia pseudotuberculosis* delivering *Yersinia pestis* LcrV and F1 antigens in mice and rats against pneumonic plague. Infect Immun 90: e0016522. [PubMed: 35900096]
18. Sun W, Six D, Kuang XY, Roland KL, Raetz CRH, and Curtiss R III. 2011. A live attenuated strain of *Yersinia pestis* KIM as a vaccine against plague. Vaccine 29: 2986–2998. [PubMed: 21320544]
19. Straley SC, and Bowmer WS. 1986. Virulence genes regulated at the transcriptional level by Ca^{2+} in *Yersinia pestis* include structural genes for outer membrane proteins. Infect Immun 51: 445–454. [PubMed: 3002984]
20. Gong S, Bearden SW, Geoffroy VA, Fetherston JD, and Perry RD. 2001. Characterization of the *Yersinia pestis* Yfu ABC inorganic iron transport system. Infect Immun 69: 2829–2837. [PubMed: 11292695]
21. Sun W, Sanapala S, Rahav H, and Curtiss R 3rd. 2015. Oral administration of a recombinant attenuated *Yersinia pseudotuberculosis* strain elicits protective immunity against plague. Vaccine 33: 6727–6735. [PubMed: 26514425]

22. Pinschewer DD, Ochsenbein AF, Odermatt B, Brinkmann V, Hengartner H, and Zinkernagel RM. 2000. FTY720 immunosuppression impairs effector T cell peripheral homing without affecting induction, expansion, and memory. J Immunol 164: 5761–5770. [PubMed: 10820254]

23. Anderson KG, Mayer-Barber K, Sung H, Beura L, James BR, Taylor JJ, Qunaj L, Griffith TS, Vezys V, Barber DL, and Masopust D. 2014. Intravascular staining for discrimination of vascular and tissue leukocytes. Nat Protoc 9: 209–222. [PubMed: 24385150]

24. Blumenthal D, Chandra V, Avery L, and Burkhardt JK. 2020. Mouse T cell priming is enhanced by maturation-dependent stiffening of the dendritic cell cortex. Elife 9.

25. Smith NM, Wasserman GA, Coleman FT, Hilliard KL, Yamamoto K, Lipsitz E, Malley R, Dooms H, Jones MR, Quinton LJ, and Mizgerd JP. 2018. Regionally compartmentalized resident memory T cells mediate naturally acquired protection against pneumococcal pneumonia. Mucosal Immunol 11: 220–235. [PubMed: 28513594]

26. Laidlaw BJ, Zhang NZ, Marshall HD, Staron MM, Guan TX, Hu YH, Cauley LS, Craft J, and Kaech SM. 2014. CD4(+) T cell help guides formation of CD103(+) lung-resident memory CD8(+) T cells during influenza viral infection. Immunity 41: 633–645. [PubMed: 25308332]

27. Turner DL, Bickham KL, Thome JJ, Kim CY, D'Ovidio F, Wherry EJ, and Farber DL. 2014. Lung niches for the generation and maintenance of tissue-resident memory T cells. Mucosal Immunol 7: 501–510. [PubMed: 24064670]

28. Wang X, Li P, Singh AK, Zhang X, Guan Z, Curtiss R 3rd, and Sun W. 2022. Remodeling *Yersinia pseudotuberculosis* to generate a highly immunogenic outer membrane vesicle vaccine against pneumonic plague. Proc Natl Acad Sci U S A 119: e2109667119. [PubMed: 35275791]

29. Sivaraman V, Pechous RD, Stasulli NM, Eichelberger KR, Miao EA, and Goldman WE. 2015. *Yersinia pestis* activates both IL-1beta and IL-1 receptor antagonist to modulate lung inflammation during pneumonic plague. PLoS Pathog 11: e1004688. [PubMed: 25781467]

30. Vesely MCA, Pallis P, Bielecki P, Low JS, Zhao J, Harman CCD, Kroehling L, Jackson R, Bailis W, Licona-Limon P, Xu H, Iijima N, Pillai PS, Kaplan DH, Weaver CT, Kluger Y, Kowalczyk MS, Iwasaki A, Pereira JP, Esplugues E, Gagliani N, and Flavell RA. 2019. Effector T(H)17 cells give rise to long-lived TRM cells that are essential for an immediate response against bacterial infection. Cell 178: 1176–1188. [PubMed: 31442406]

31. Bi YJ, Zhou JY, Yang H, Wang X, Zhang XC, Wang Q, Wu XH, Han YP, Song YJ, Tan YF, Du ZM, Yang HY, Zhou DS, Cui YJ, Zhou L, Yan YF, Zhang PP, Guo ZB, Wang XY, Liu GW, and Yang RF. 2014. IL-17A produced by neutrophils protects against pneumonic plague through orchestrating IFN-gamma-activated Macrophage programming. J Immunol 192: 704–713. [PubMed: 24337746]

32. Allen AC, Wilk MM, Misiak A, Borkner L, Murphy D, and Mills KHG. 2018. Sustained protective immunity against *Bordetella pertussis* nasal colonization by intranasal immunization with a vaccine-adjuvant combination that induces IL-17-secreting T-RM cells. Mucosal Immunol 11: 1763–1776. [PubMed: 30127384]

33. Uddback I, Cartwright EK, Scholler AS, Wein AN, Hayward SL, Lobby J, Takamura S, Thomsen AR, Kohlmeier JE, and Christensen JP. 2021. Long-term maintenance of lung resident memory T cells is mediated by persistent antigen. Mucosal Immunol 14: 92–99. [PubMed: 32518368]

34. Parent MA, Berggren KN, Kummer LW, Wilhelm LB, Szaba FM, Mullarky IK, and Smiley ST. 2005. Cell-mediated protection against pulmonary *Yersinia pestis* infection. Infect Immun 73: 7304–7310. [PubMed: 16239527]

35. Dinc G, Pennington JM, Yolcu ES, Lawrenz MB, and Shirwan H. 2014. Improving the Th1 cellular efficacy of the lead *Yersinia pestis* rF1-V subunit vaccine using SA-4-1BBL as a novel adjuvant. Vaccine 32: 5035–5040. [PubMed: 25045812]

36. Williamson ED, Eley SM, Stagg AJ, Green M, Russell P, and Titball RW. 2000. A single dose sub-unit vaccine protects against pneumonic plague. Vaccine 19: 566–571. [PubMed: 11027822]

37. Powell BS, Andrews GP, Enama JT, Jendrek S, Bolt C, Worsham P, Pullen JK, Ribot W, Hines H, Smith L, Heath DG, and Adamovicz JJ. 2005. Design and testing for a nontagged F1-V fusion protein as vaccine antigen against bubonic and pneumonic plague. Biotechnol Prog 21: 1490–1510. [PubMed: 16209555]

38. Smiley ST 2008. Current challenges in the development of vaccines for pneumonic plague. Expert review of vaccines 7: 209–221. [PubMed: 18324890]
39. Quenee LE, Ciletti NA, Elli D, Hermanas TM, and Schneewind O. 2011. Prevention of pneumonic plague in mice, rats, guinea pigs and non-human primates with clinical grade rV10, rV10-2 or F1-V vaccines. Vaccine 29: 6572–6583. [PubMed: 21763383]
40. Wang X, Singh AK, Zhang X, and Sun W. 2020. Induction of protective anti-plague immune responses by self-adjuvanting bionanoparticles derived from engineered *Yersinia pestis*. Infect Immun 88: e00081–00020. [PubMed: 32152195]
41. Cote CK, Biryukov SS, Klimko CP, Shoe JL, Hunter M, Rosario-Acevedo R, Fetterer DP, Moody KL, Meyer JR, Rill NO, Dankmeyer JL, Worsham PL, Bozue JA, and Welkos SL. 2021. Protection Elicited by Attenuated Live *Yersinia pestis* Vaccine Strains against Lethal Infection with Virulent *Y. pestis*. Vaccines (Basel) 9.
42. Autenrieth IB, Tingle A, Reske-Kunz A, and Heesemann J. 1992. T lymphocytes mediate protection against *Yersinia enterocolitica* in mice: characterization of murine T-cell clones specific for *Y. enterocolitica*. Infect Immun 60: 1140–1149. [PubMed: 1541529]
43. Russmann H, Gerdemann U, Igwe EI, Panthel K, Heesemann J, Garbom S, Wolf-Watz H, and Geginat G. 2003. Attenuated *Yersinia pseudotuberculosis* carrier vaccine for simultaneous antigen-specific CD4 and CD8 T-cell induction. Infect Immun 71: 3463–3472. [PubMed: 12761131]
44. Downey-Slinker ED, Ridpath JF, Sawyer JE, Skow LC, and Herring AD. 2016. Antibody titers to vaccination are not predictive of level of protection against a BVDV type 1 b challenge in Bos indicus - Bos taurus steers. Vaccine 34: 5053–5059. [PubMed: 27601344]
45. Scepanovic P, Alanio C, Hammer C, Hodel F, Bergstedt J, Patin E, Thorball CW, Chaturvedi N, Charbit B, Abel L, Quintana-Murci L, Duffy D, Albert ML, Fellay J, and Milieu Interieur C. 2018. Human genetic variants and age are the strongest predictors of humoral immune responses to common pathogens and vaccines. Genome Med 10: 59. [PubMed: 30053915]
46. Criscuolo E, Diotti RA, Strollo M, Rolla S, Ambrosi A, Locatelli M, Burioni R, Mancini N, Clementi M, and Clementi N. 2021. Weak correlation between antibody titers and neutralizing activity in sera from SARS-CoV-2 infected subjects. J Med Virol 93: 2160–2167. [PubMed: 33064340]
47. Masopust D, and Soerens AG. 2019. Tissue-Resident T cells and other resident leukocytes. Annu Rev Immunol 37: 521–546. [PubMed: 30726153]
48. Zheng MZM, and Wakim LM. 2021. Tissue resident memory T cells in the respiratory tract. Mucosal Immunol.
49. Morabito KM, Ruckwardt TR, Redwood AJ, Moin SM, Price DA, and Graham BS. 2017. Intranasal administration of RSV antigen-expressing MCMV elicits robust tissue-resident effector and effector memory CD8+ T cells in the lung. Mucosal Immunol 10: 545–554. [PubMed: 27220815]
50. Schenkel JM, and Masopust D. 2014. Tissue-resident memory T cells. Immunity 41: 886–897. [PubMed: 25526304]
51. Perdomo C, Zedler U, Kuhl AA, Lozza L, Saikali P, Sander LE, Vogelzang A, Kaufmann SH, and Kupz A. 2016. Mucosal BCG vaccination induces protective lung-resident memory T cell populations against tuberculosis. mBio 7.
52. Wakim LM, Gebhardt T, Heath WR, and Carbone FR. 2008. Cutting edge: local recall responses by memory T cells newly recruited to peripheral nonlymphoid tissues. J Immunol 181: 5837–5841. [PubMed: 18941171]
53. Khan TN, Mooster JL, Kilgore AM, Osborn JF, and Nolz JC. 2016. Local antigen in nonlymphoid tissue promotes resident memory CD8+ T cell formation during viral infection. J Exp Med 213: 951–966. [PubMed: 27217536]
54. Szabo PA, Miron M, and Farber DL. 2019. Location, location, location: Tissue resident memory T cells in mice and humans. Sci Immunol 4.
55. Philipovskiy AV, and Smiley ST. 2007. Vaccination with live *Yersinia pestis* primes CD4 and CD8 T cells that synergistically protect against lethal pulmonary *Y. pestis* infection. Infect Immun 75: 878–885. [PubMed: 17118978]

56. Szaba FM, Kummer LW, Duso DK, Koroleva EP, Tumanov AV, Cooper AM, Bliska JB, Smiley ST, and Lin JS. 2014. TNFalpha and IFNgamma but not perforin are critical for CD8 T cell-mediated protection against pulmonary *Yersinia pestis* infection. PLoS Pathog 10: e1004142. [PubMed: 24854422]
57. Ugur M, Schulz O, Menon MB, Krueger A, and Pabst O. 2014. Resident CD4+ T cells accumulate in lymphoid organs after prolonged antigen exposure. Nat Commun 5: 4821. [PubMed: 25189091]
58. Schenkel JM, Fraser KA, and Masopust D. 2014. Cutting edge: resident memory CD8 T cells occupy frontline niches in secondary lymphoid organs. J Immunol 192: 2961–2964. [PubMed: 24600038]
59. Takamura S 2018. Niches for the long-term maintenance of tissue-resident memory T cells. Front Immunol 9: 1214. [PubMed: 29904388]
60. Beura LK, Wijeyesinghe S, Thompson EA, Macchietto MG, Rosato PC, Pierson MJ, Schenkel JM, Mitchell JS, Vezys V, Fife BT, Shen S, and Masopust D. 2018. T cells in nonlymphoid tissues give rise to lymph-node-resident memory T Cells. Immunity 48: 327-+. [PubMed: 29466758]
61. Yang QT, Zhang MX, Chen Q, Chen WX, Wei CL, Qiao K, Ye TS, Deng GF, Li J, Zhu JL, Cai Y, Chen XC, and Ma L. 2020. Cutting Edge: characterization of human tissue-resident memory T cells at different infection sites in patients with tuberculosis. J Immunol 204: 2331–2336. [PubMed: 32229539]
62. Oja AE, Piet B, Helbig C, Stark R, van der Zwan D, Blaauwgeers H, Remmerswaal EBM, Amsen D, Jonkers RE, Moerland PD, Nolte MA, van Lier RAW, and Hombrink P. 2018. Trigger-happy resident memory CD4(+) T cells inhabit the human lungs. Mucosal Immunol 11: 654–667. [PubMed: 29139478]
63. Zhao Y, Yang Q, Jin C, Feng Y, Xie S, Xie H, Qi Y, Qiu H, Chen H, Tao A, Mu J, Qin W, and Huang J. 2019. Changes of CD103-expressing pulmonary CD4(+) and CD8(+) T cells in *S. japonicum* infected C57BL/6 mice. BMC Infect Dis 19: 999. [PubMed: 31775660]
64. Alspach E, Lussier DM, and Schreiber RD. 2019. Interferon gamma and Its important roles in promoting and inhibiting spontaneous and therapeutic cancer immunity. Cold Spring Harb Perspect Biol 11.
65. Nandi B, and Behar SM. 2011. Regulation of neutrophils by interferon-gamma limits lung inflammation during tuberculosis infection. J Exp Med 208: 2251–2262. [PubMed: 21967766]
66. Tsai HC, Velichko S, Hung LY, and Wu R. 2013. IL-17A and Th17 cells in lung inflammation: an update on the role of Th17 cell differentiation and IL-17R signaling in host defense against infection. Clin Dev Immunol 2013: 267971. [PubMed: 23956759]
67. Ross PJ, Sutton CE, Higgins S, Allen AC, Walsh K, Misiak A, Lavelle EC, McLoughlin RM, and Mills KH. 2013. Relative contribution of Th1 and Th17 cells in adaptive immunity to *Bordetella pertussis*: towards the rational design of an improved acellular pertussis vaccine. PLoS Pathog 9: e1003264. [PubMed: 23592988]
68. Ueno K, Urai M, Sadamoto S, Shinozaki M, Takatsuka S, Abe M, Otani Y, Yanagihara N, Shimizu K, Iwakura Y, Shibuya K, Miyazaki Y, and Kinjo Y. 2019. A dendritic cell-based systemic vaccine induces long-lived lung-resident memory Th17 cells and ameliorates pulmonary mycosis. Mucosal Immunol 12: 265–276. [PubMed: 30279512]
69. Kirchner FR, and LeibundGut-Landmann S. 2021. Tissue-resident memory Th17 cells maintain stable fungal commensalism in the oral mucosa. Mucosal Immunol 14: 455–467. [PubMed: 32719409]

Key points:

1. Oral Yptb1(pYA5199) vaccination developed lung resident memory T cells (T_{RM})
2. Lung T_{RM} expressed IFN-γ and IL-17A played a vital role against pneumonic plague.
3. Oral Yptb1(pYA5199) vaccination developed long-lived immunity in the lung.

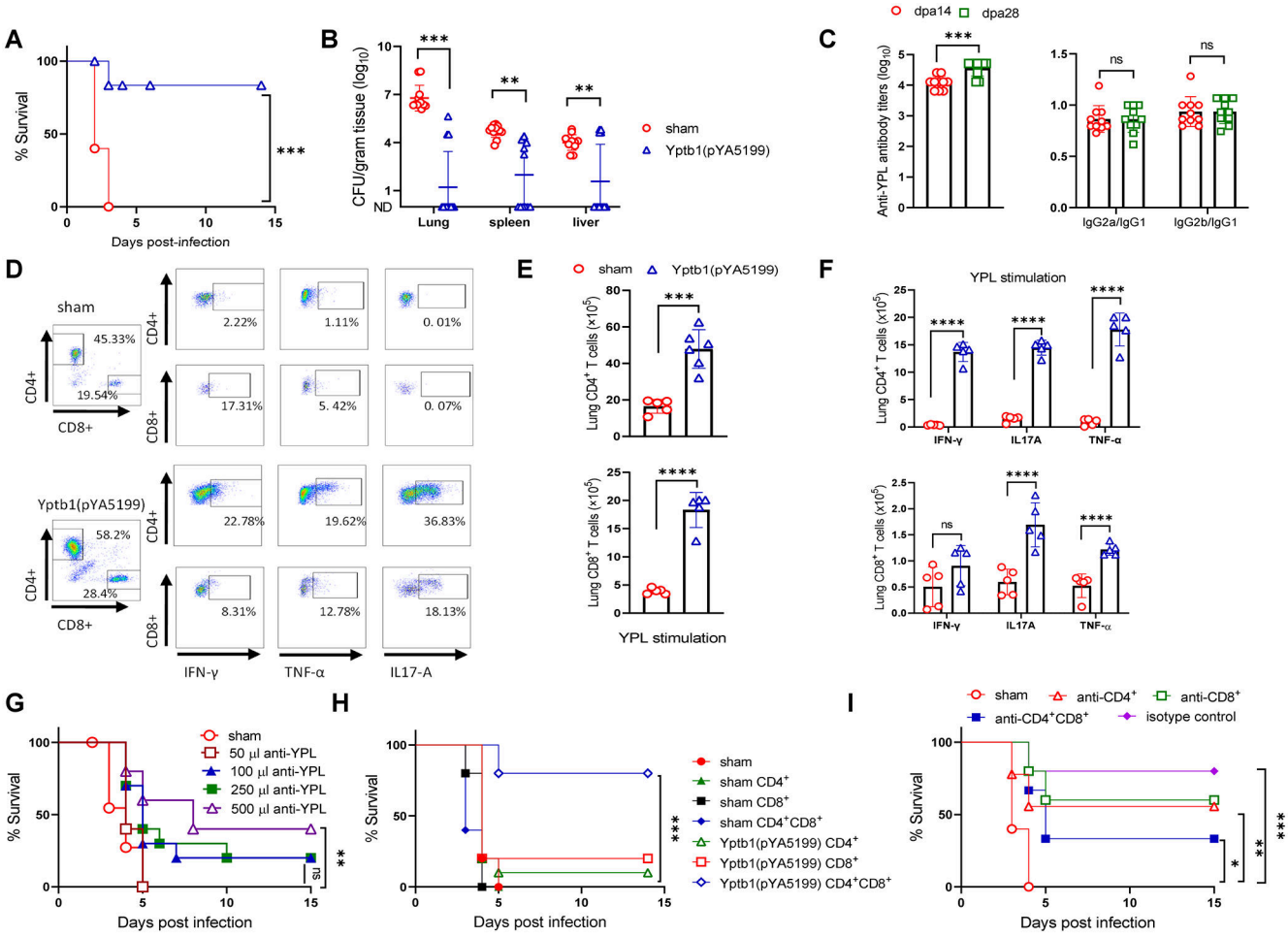

Figure 1. Oral immunization with the Yptb1(pYA5199) vaccine confers T cell-mediated comprehensive protection against pneumonic *Y. pestis* infection.

(A) On the 42nd day after immunization, mice (n=15, mixed males and females) were intranasally challenged with 5×10^3 CFU (50 LD_{50}) of *Y. pestis* KIM6+(pCD1Ap). Survival was recorded for 14 dpi. (B) The bacterial burden in the lung, spleen, and liver at 2 dpi. (C) Antibody responses. Serum anti-YPL antibody titers in immunized mice at 14 and 28 dpv [left]; the ratios of IgG2a/IgG1 and IgG2b/IgG1 to YPL [right]. (D) Representative flow plots showing the frequency of lung $CD4^+$ and $CD8^+$ T cells and the respective cells producing IFN-γ, TNF-α, or IL-17A in mice (n=6 females). (E) At dpv 42, lung single cells obtained from Yptb1(pYA5199) and sham mice were *in vitro* stimulated for 72 h with YPL. The absolute number of lung $CD4^+$ and $CD8^+$ T cells and (F) lung T cells expressing IFN-γ, TNF-α, or IL-17A were determined by Flow cytometer. (G) Serum transfer. Naïve mice (n=10, females) were i.p. injected with different volumes of serum collected from sham and Yptb1(pYA5199)-immunized mice at 42 dpv. Twenty-four hours post-injection, recipient mice were intranasally challenged with 10 LD_{50} of *Y. pestis*. (H) Lung T-cell transfer. Naïve mice treated with a single dose of irradiation (5 Gy) were intravenously administered $CD4^+$ and/or $CD8^+$ T cells (2×10^6 cells/mouse) isolated from sham or Yptb1(pYA5199)-immunized mice at 42 dpv. At 24 h post-administration, mice (n=10, females) were intranasally infected with 10 LD_{50} of *Y. pestis,* and survival was monitored

for 14 days. (I) T-cell depletion. Mice (n=10, females) were depleted of $CD4^+$ and/or $CD8^+$ T cells by i.p. administration of anti-CD4, anti-CD8, or anti-CD4 plus anti-CD8 monoclonal antibodies (500 μg/each mouse in 200 μl) and then intranasally challenged with 50 LD_{50} of *Y. pestis*. Each symbol in the individual bar graph represents a data point obtained from an individual mouse. Each experiment was performed two times with identical conditions. Data obtained from experiments were pooled and analyzed and are presented as the mean ± SD. The statistical analysis is described in the Materials and Methods.

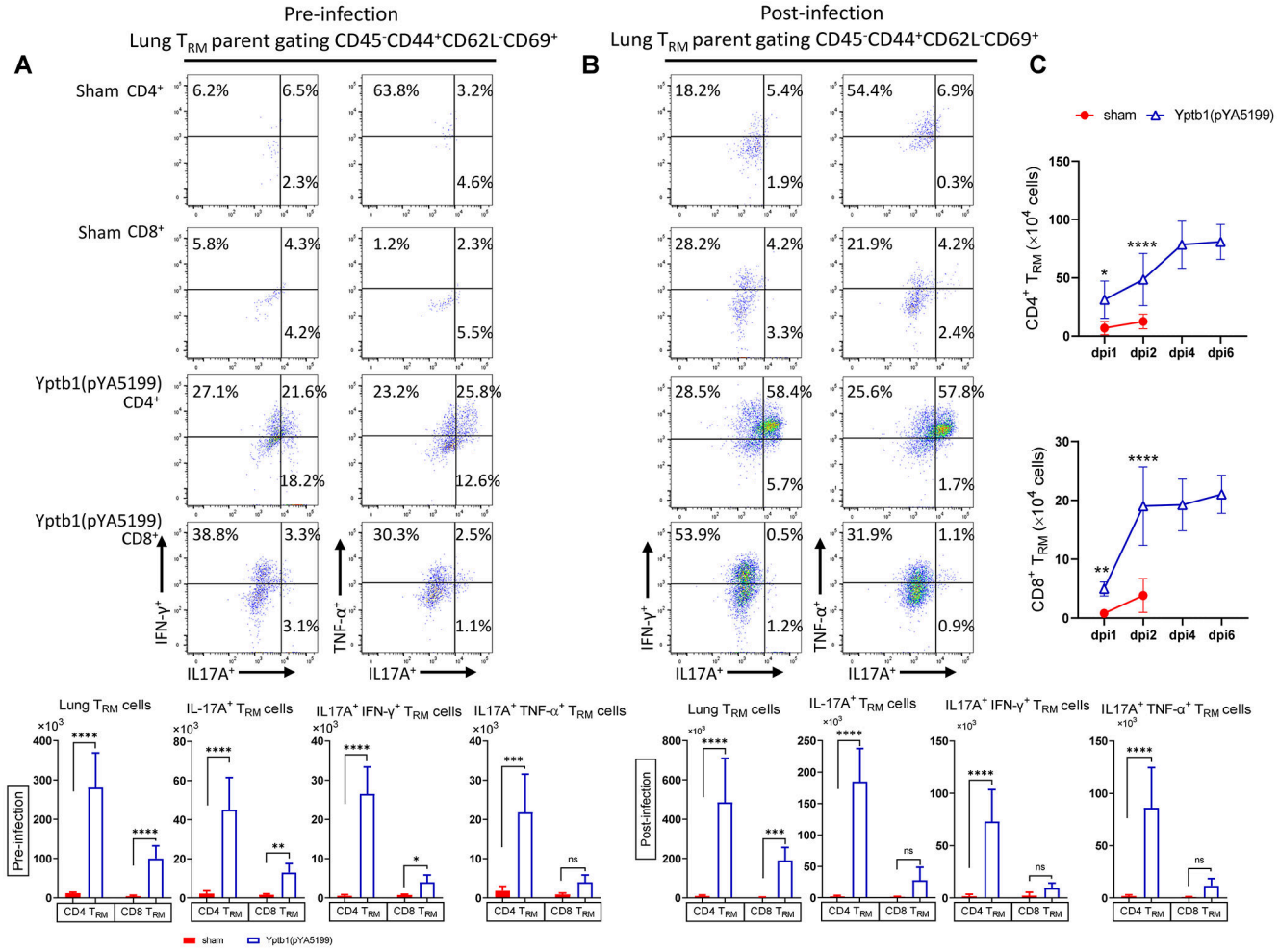

Figure 2. Lung CD4$^+$ and CD8$^+$ T_{RM} cells are activated by oral Yptb1(pYA5199) immunization and expand after pulmonary *Y. pestis* infection.

Mice were intravenously injected via the tail vein with 5 μg of FITC-conjugated anti-CD45.2 mAbs diluted in 200 μl of sterile PBS to distinguish lung T_{RM} cells from circulating T cells. Five minutes post-injection, mice were euthanized to isolate lung single cells (n=5 females). Lung cells isolated from Yptb1(pYA5199)-immunized and sham mice were *in vitro* stimulation with PMA+ ionomycin. (A) Representative flow plots of lung CD4$^+$ and CD8$^+$ T_{RM} cells producing IFN-γ, TNF-α, and/or IL-17A in immunized and sham mice at 42 dpv. Lung T_{RM} cells were gated based on CD45$^-$ (i.v. injection), CD4$^+$/CD8$^+$, CD44$^+$, and CD69$^+$, as well as intracellular cytokines (IFN-γ$^+$, TNF-α$^+$, and IL-17A$^+$), in the flow cytometry protocol [top]. Quantitative analysis of the number of lung CD4$^+$ or CD8$^+$ T_{RM} cells and corresponding cells producing IFN-γ, TNF-α, and/or IL-17A [bottom]. (B) Representative flow plots of lung CD4$^+$ and CD8$^+$ T_{RM} cells in mice at 2 dpi [top]. Quantitative analysis of the number of lung CD4$^+$ or CD8$^+$ T_{RM} cells and corresponding cells producing IFN-γ, TNF-α, and/or IL-17A (bottom) (n=10 females). (C) Kinetic analysis of lung CD4$^+$ and CD8$^+$ T_{RM} cells after pulmonary *Y. pestis* infection (n=10 females). Data obtained from a minimum of two experiments are presented as the mean ± SD. The statistical analysis is described in the Materials and Methods.

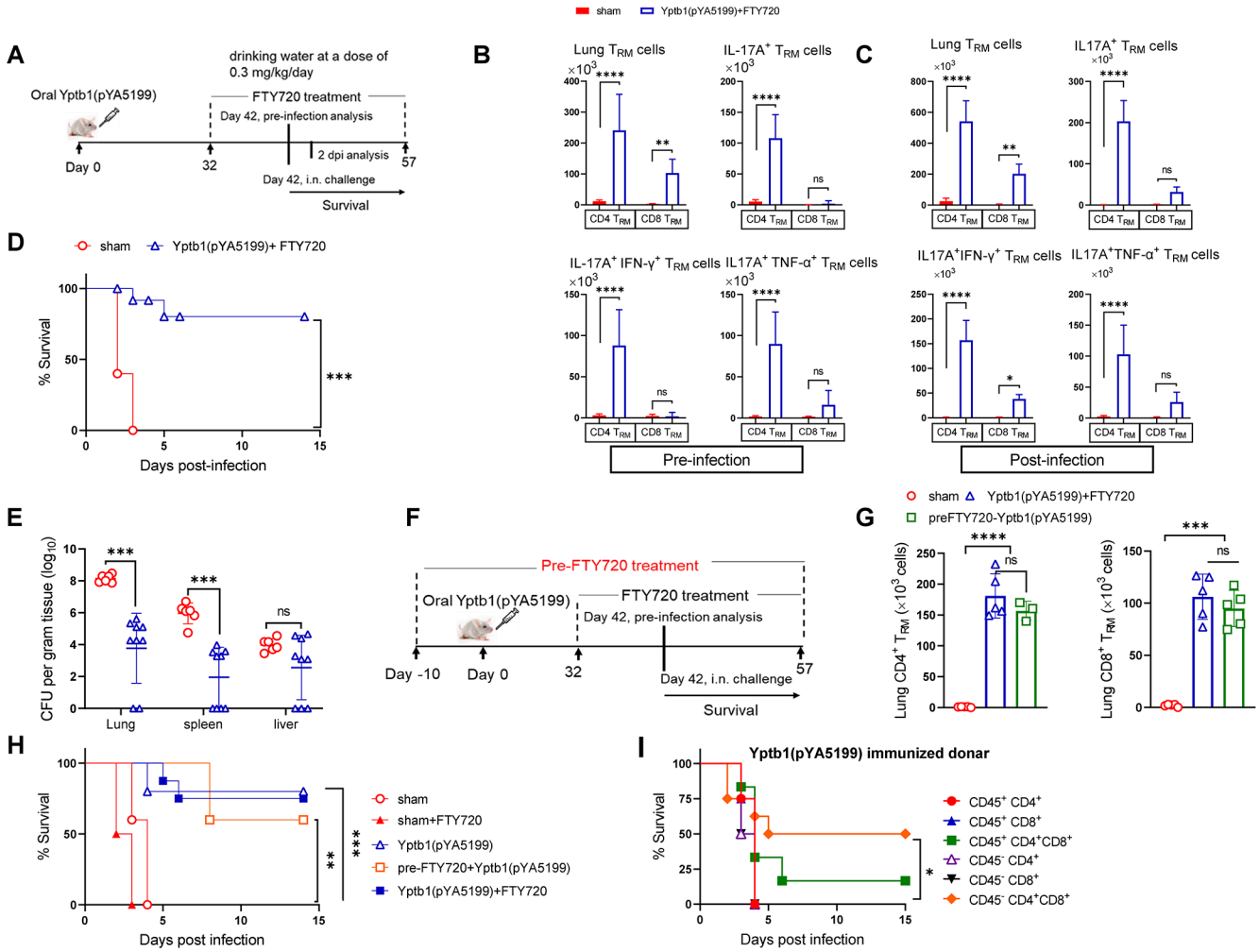

Figure 3. CD4$^+$ and CD8$^+$ T_{RM} cells established in the lungs of FTY720-treated Yptb1(pYA5199)-immunized mice offer protection against pulmonary *Y. pestis* infection.

(A) Scheme of the immunization, FTY720 treatment, T_{RM} cell analysis, and *Y. pestis* infection. The lung single cell isolated Yptb1(pYA5199)+FTY720 immunized and sham mice were *in vitro* stimulated with PMA+ionomycine. (B) Quantitative analysis of the number of lung CD4$^+$ or CD8$^+$ T_{RM} cells and corresponding cells producing IFN-γ, TNF-α, and/or IL-17A in FTY720-treated Yptb1(pYA5199)-immunized mice at 42 dpv (n=5 females). (C) Quantitative analysis of the number of lung CD4$^+$ or CD8$^+$ T_{RM} cells and corresponding cells producing IFN-γ, TNF-α, and/or IL-17A in FTY720-treated Yptb1(pYA5199)-immunized mice at 2 dpi. (D) On 42 dpv, FTY720-treated Yptb1(pYA5199)-immunized mice (n=15, mixed males and females) were intranasally challenged with 50 LD_{50} of *Y. pestis*. Survival was recorded for 14 days. (E) The bacterial burden was evaluated in the lung, spleen, and liver at 2 dpi (n=6, mixed males and females). (F) Scheme of the FTY720 treatment 10 days before oral Yptb1(pYA5199) immunization and until the end of the experiment. (G) Quantitative analysis of the number of lung CD4$^+$ or CD8$^+$ T_{RM} cells in pre- and post-FTY720-treated Yptb1(pYA5199)-immunized mice at 42 dpv. (H) On 42 dpv, mice (n=5, mixed males and females) were intranasally challenged with 50 LD_{50} of *Y. pestis*. (I) Adoptive transfer of FACS-sorted lung circulating (CD45$^+$) T cells

or T_{RM} cells ($CD45^{-}$) from Yptb1(pYA5199)-immunized mice. Sorted cells were injected into irradiated (5 Gy) naïve mice via the intratracheal route. At 24 h after administration, recipient mice (n=10 females) were i.n. challenged with 10 LD_{50} of *Y. pestis*. In the bar plots, each symbol represents a data point obtained from an individual mouse. Data are presented as the mean ± SD. The statistical analysis is described in the Materials and Methods.

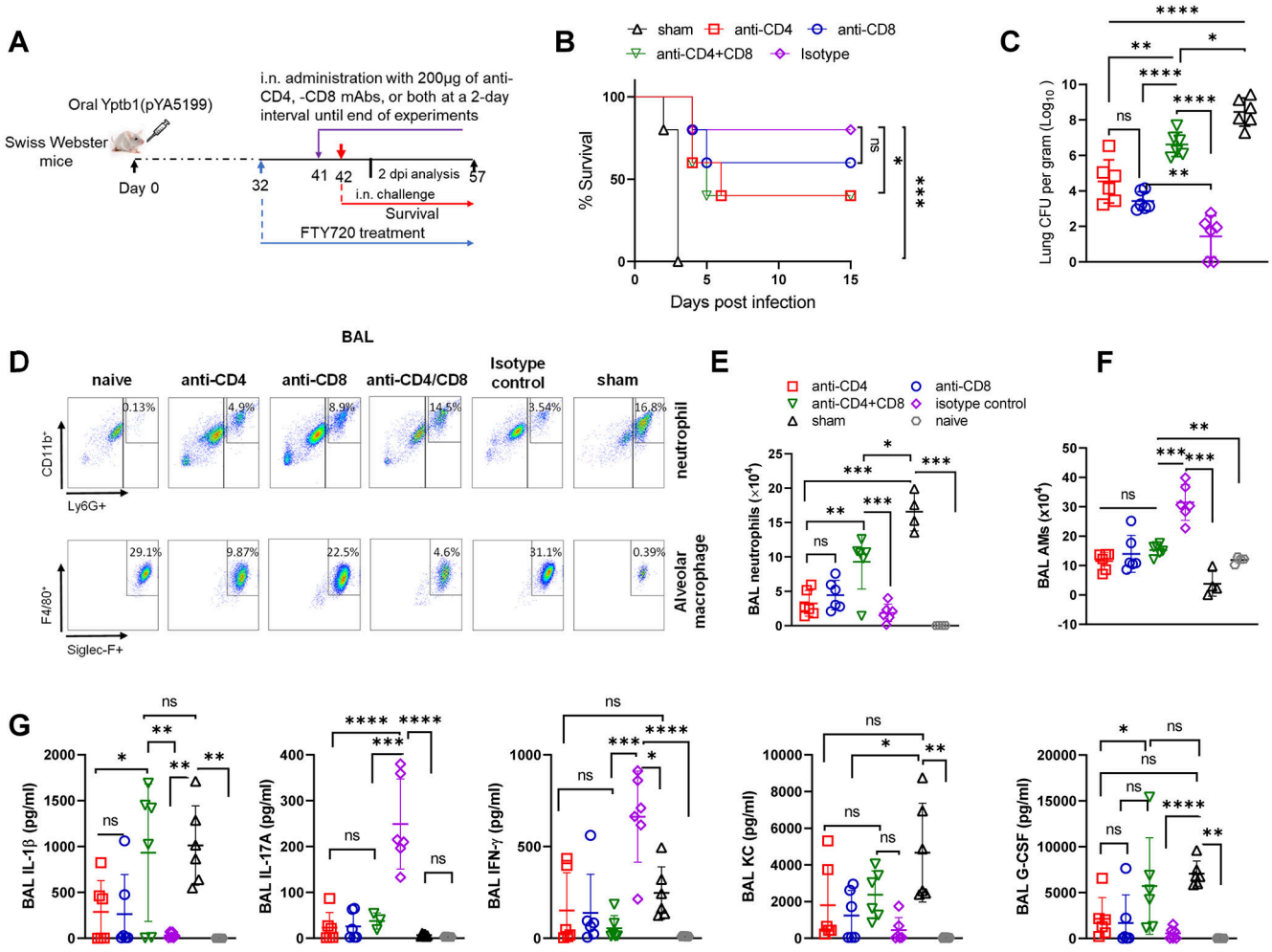

Figure 4. Local depletion of lung resident CD4$^+$ and/or CD8$^+$ T cells in Yptb1(pYA5199)-immunized mice impairs protection against pneumonic plague.

(A) Scheme of immunization, FTY720 treatment, T-cell depletion, and survival against pneumonic plague infection. (B) Survival study in the lung T cell-depleted mice. The Yptb1(pYA5199)+FTY720-immunized mice (n=6 females) were depleted of CD4$^+$ and/or CD8$^+$ T cells at the lung mucosal site by i.n. administration of 200 µg of anti-CD4, anti-CD8, or both mAbs and then intranasally challenged with 50 LD_{50} of *Y. pestis*. (C) Lung *Y. pestis* burden at 2 dpi (n= 5 females). (D) Representative flow plots showing the percentages of neutrophils and alveolar macrophages in the BAL fluid at 2 dpi. (E) The number of neutrophils and (F) alveolar macrophages (AMs) in the BAL fluid of control and T cell-depleted mice (n= 6 females) at 2 dpi. (G) Analysis of cytokines and chemokines in the BAL fluid samples collected at 2 dpi. Each symbol represents a data point obtained from an individual mouse. The statistical analysis is described in the Materials and Methods.

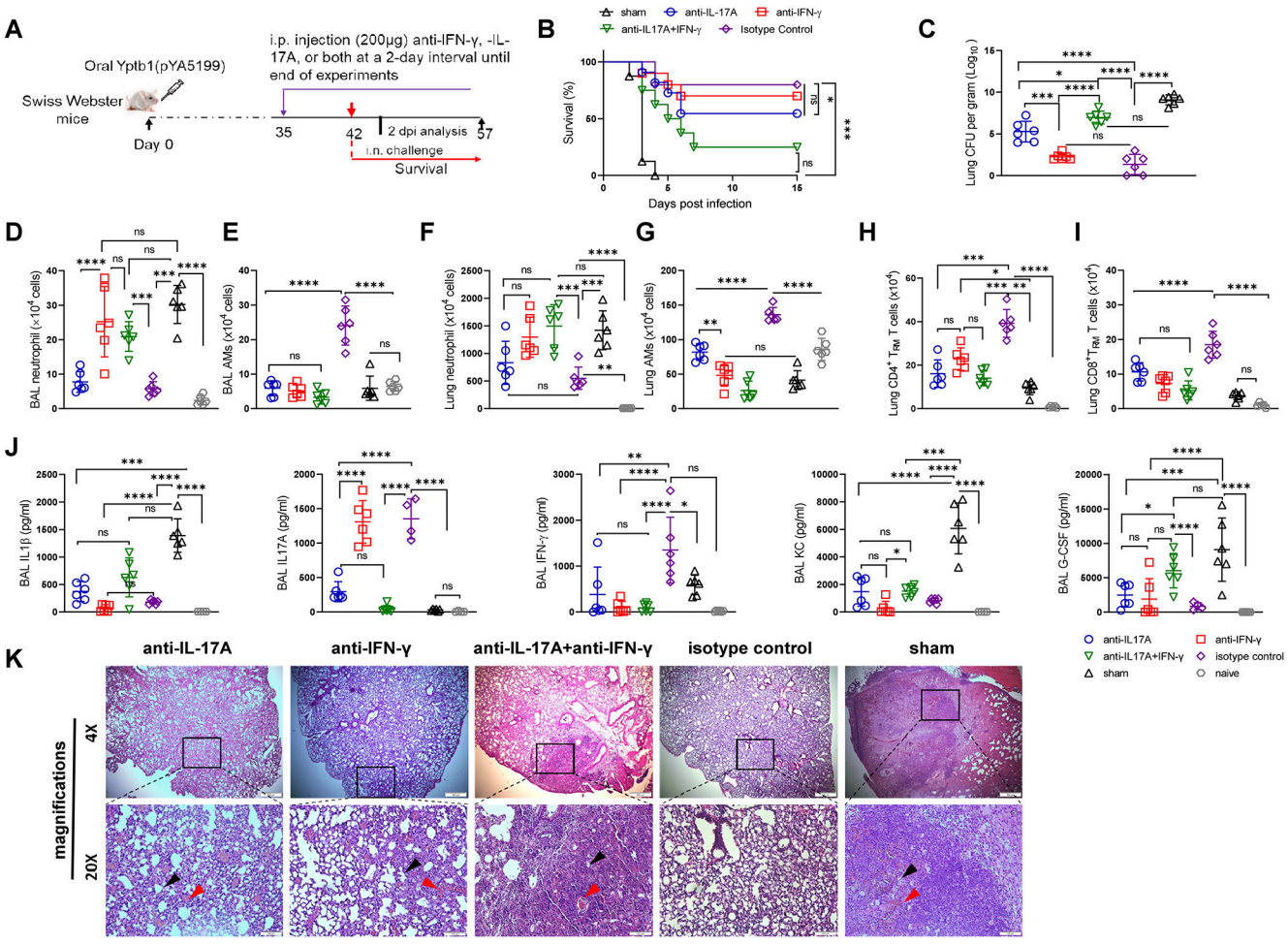

Figure 5. IFN-γ and IL-17A play a critical role in protection against pulmonary *Y. pestis* challenge.

(A) Scheme of neutralization of IFN-γ, IL-17A, or both in Yptb1(pYA5199)-immunized mice. Mice administrated with PBS (sham) were used as control. (B) Survival study with cytokine neutralization. The Yptb1(pYA5199)-immunized mice (n=10 females) were intraperitoneally injected with 200 µg of anti-IFN-γ, anti-IL-17A, or both mAbs and then intranasally challenged with 50 LD_{50} of *Y. pestis*. (C) Lung *Y. pestis* burden in the respective group of mice at 2 dpi. (D) The number of neutrophils and (E) AMs in the BAL fluid. (F) The absolute number of lung neutrophil and (G) AMs in the lung of mice (n=6 females) treated with anti-IFN-γ, anti-IL-17A, anti-IFN-γ/IL-17A, or isotype control antibodies at 2 dpi. (H) The number of $CD4^+$ and (I) $CD8^+$ T_{RM} cells in the lungs of mice (n=6 females) treated with the respective antibodies at 2 dpi. (J) Analysis of cytokines and chemokines in the BAL fluid of mice (n=6 females) treated with the respective antibodies at 2 dpi. (K) Representative H&E-stained lung sections of oral Yptb1(pYA5199)-immunized mice treated with anti-IFN-γ, anti-IL-17A, anti-IFN-γ/IL-17A or isotype control antibodies, or sham mice collected at 2 dpi. The black arrow indicates a reduced alveolar lacunar space, while the red arrow indicates a lung lesion or hemorrhage. Each symbol represents a data point obtained from an individual mouse. Data are presented as the mean ± SD. The statistical analysis is described in the Materials and Methods.

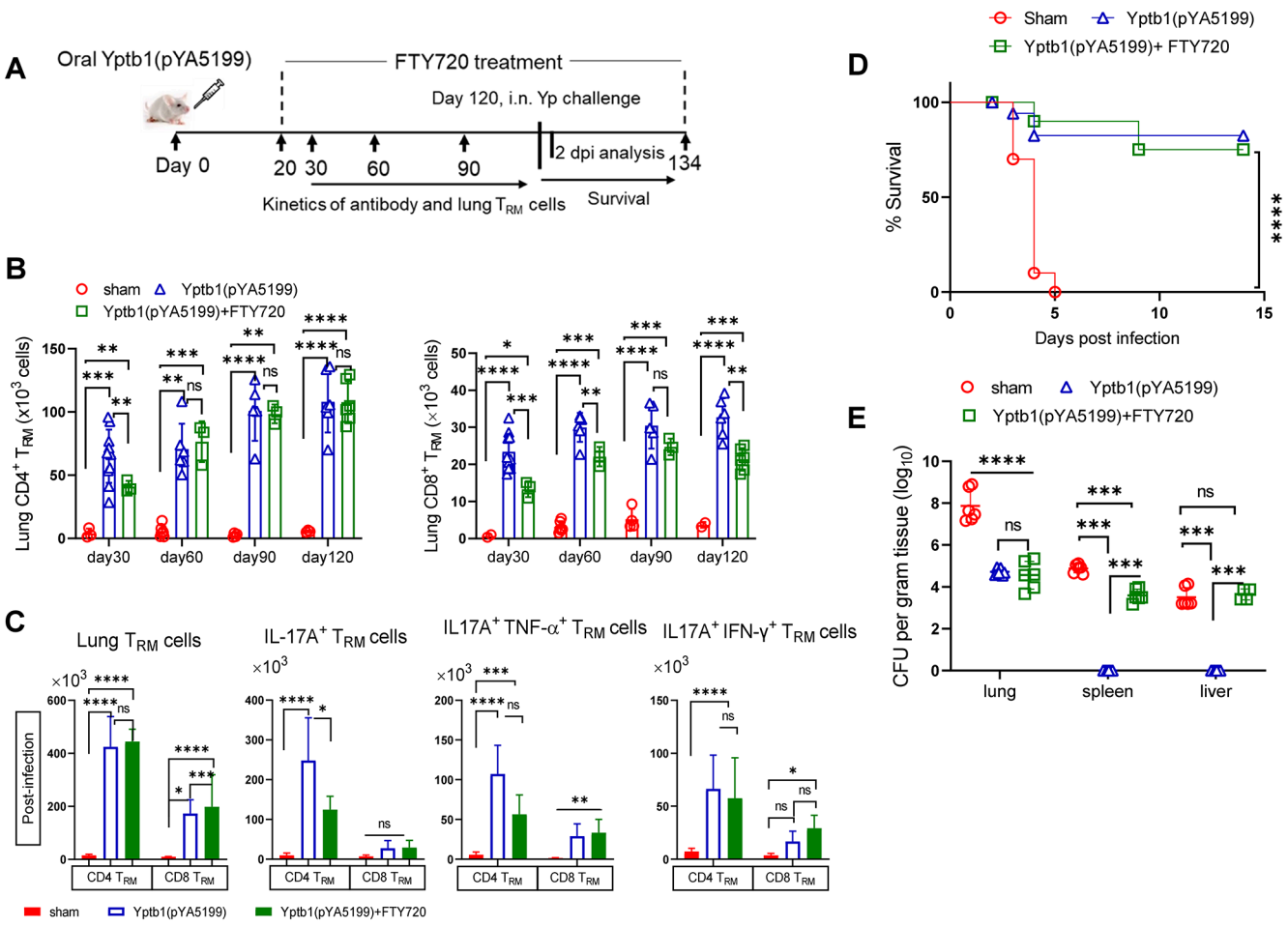

Figure 6. Lung T_{RM} cells activated by oral Yptb1(pYA5199) immunization confer long-lasting protection.

(A) Scheme of the immunization, immune parameter analysis, and challenge in the long-term animal study. (B) Kinetic analysis of lung $CD4^+$ and $CD8^+$ T_{RM} cells in Yptb1(pYA5199)-immunized mice treated with or without FTY720 at 30, 60, 90, and 120 dpv. (n=6 females) (C) Mice were intravenously injected via the tail vein with 5 μg of FITC-conjugated anti-CD45.2 mAbs diluted in 200 μl of sterile PBS to distinguish lung T_{RM} cells from circulating T cells. Five minutes post-injection, mice were euthanized to isolate lung single cells (n=5 females). Lung cells isolated from Yptb1(pYA5199), Yptb1(pYA5199)+FTY720 immunized and sham mice were *in vitro* stimulation with PMA+ ionomycin. Quantitative analysis of the number of lung $CD4^+$ or $CD8^+$ T_{RM} cells and corresponding cells producing IFN-γ, TNF-α, and/or IL-17A in Yptb1(pYA5199)-immunized mice treated with or without FTY720 and control mice was performed at 2 dpi. (D) On the 120th day after immunization, mice (n=10, equal number of males and females) were intranasally challenged with 50 LD_{50} of *Y. pestis*. (E) The bacterial burden was evaluated in the lung, liver, and spleen of mice (n=6, mixed males and females) at 2 dpi. Data obtained from experiments are presented as the mean ± SD. The statistical analysis is described in Materials and Methods.